Article:

Wang, Y., Liu, Z. and Brindley, P. (2026) Understanding the cooling mechanisms of urban canal-edge walkways through blue–green infrastructure: a parametric ENVI-met study. Urban Science, 10 (9). 509. ISSN: 2413-8851

https://doi.org/10.3390/urbansci10090509 *urban science*

MDPI

Article

Understanding the Cooling Mechanisms of Urban Canal-Edge Walkways Through Blue–Green Infrastructure: A Parametric ENVI-Met Study

Yuqi Wang, Zhixin Liu * and Paul Brindley

School of Architecture and Landscape, The University of Sheffield, Sheffield S10 2TN, UK;
yw951228@gmail.com (Y.W.); p.brindley@sheffield.ac.uk (P.B.)
* Correspondence: zhixin.liu@sheffield.ac.uk

Abstract

Urban canal-edge spaces are increasingly recognised as important blue–green infrastructure for mitigating urban heat; however, the mechanisms governing pedestrian thermal comfort in these environments remain insufficiently understood. This study employed a validated ENVI-met model to investigate the effects of canal orientation, canal width, water bodies and riparian tree configuration on pedestrian thermal comfort under summer heatwave conditions in Manchester, UK. A total of 32 scenarios were simulated to quantify the individual and combined effects of these design factors. Canal water alone provided only moderate daytime cooling, with its effectiveness depending strongly on canal orientation and local ventilation conditions. In contrast, riparian trees substantially improved thermal comfort through reductions in mean radiant temperature associated with canopy shading. Furthermore, the study identified that thermal performance was influenced not simply by the presence of blue and green infrastructure, but by their interaction. Rather than acting as the dominant cooling source, canal water enhanced the cooling effectiveness of adjacent vegetation, while continuous canopy shading emerged as the principal mechanism controlling pedestrian thermal comfort. These findings provide new insights into the mechanisms of canal-edge cooling and offer quantitative evidence to support climate-responsive design of thermally comfortable and resilient urban waterfronts.

Keywords: blue–green infrastructure; canal-edge walkways; outdoor thermal comfort; synergistic cooling; urban microclimate; ENVI-met

1. Introduction

Climate change is reshaping the thermal environments of cities worldwide, with rising temperatures increasingly posing risks to human health and urban livability. In the UK, despite its historically cool and mild climate, extreme heat events are becoming more frequent and severe. During the July 2022 heatwave, temperatures exceeded 40 °C for the first time, reaching 40.3 °C at London Heathrow and causing substantial excess mortality. This event highlights that urban heat is not merely a seasonal discomfort but a critical public health concern, increasing heat-related morbidity and mortality [1,2]. These risks are further exacerbated by the urban heat island (UHI) effect in dense urban environments [3].

The IPCC identifies urban blue–green infrastructure (BGI) as an important pathway for climate adaptation [4]. In this study, BGI is defined as a strategically planned and interconnected network of blue and green spaces, including vegetation, open spaces and water

Academic Editor: Francesco Ferrini

Received: 4 August 2026
Revised: 26 August 2026
Accepted: 27 August 2026
Published: 2 September 2026

bodies, designed and managed to deliver ecosystem services and support human well-being [5–7]. Beyond environmental benefits such as air-quality improvement, stormwater regulation and habitat connectivity, BGI is increasingly recognised for its role in urban heat adaptation, although its effectiveness depends on the spatial configuration and local context [8–10].

Canal-edge walkways, often referred to as towpaths in the UK context, are linear pedestrian or shared-use routes running alongside canals. Historically used by horses to pull cargo boats, towpaths are now managed as pedestrian-priority shared spaces that support walking, cycling, boating access, recreation and create opportunities for everyday contact with water and nature [11]. Towpaths represent a significant component of built infrastructure, with 2000 miles of towpath in England and Wales and 50% of the British population residing within 5 miles of a towpath [11,12]. UK precedents illustrate the wider design relevance of this spatial type: London's Regent's Canal has been studied as a post-industrial canal corridor where water, vegetation and linear form shape public-space experience and everyday movement [13], while Queen Elizabeth Olympic Park uses green-infrastructure and park-design guidance to frame waterways and parklands as part of a climate-resilient public realm [14,15]. These examples position canal-edge walkways as blue–green public spaces whose design value depends on how water, vegetation and linear public realm are configured for comfortable pedestrian use under heat conditions.

The thermal performance of canal-side environments is governed by interacting blue–green processes at the pedestrian scale. Water bodies contribute to cooling through evaporation and thermal storage, although the spatial extent of these effects may be limited in narrow canals [16,17]. Their cooling influence is also conditioned by surrounding airflow and urban ventilation patterns [18,19]. Compared with water bodies, vegetation generally provides greater daytime cooling through a combination of shading, evapotranspiration and modifications to local airflow [20–23]. Previous studies have demonstrated that vegetation cooling is strongly influenced by canopy structure, species characteristics and planting configuration, although reported cooling performance varies considerably among different urban contexts [3,20,24–26]. Beyond these individual effects, increasing attention has been given to the combined application of blue–green infrastructure rather than considering blue and green elements independently [27–31]. Although previous studies generally report greater cooling benefits from integrated blue–green strategies than from single-element interventions, most research has focused on parks, rivers and lakes. Comparatively little is known about narrow urban canal corridors, where spatial constraints and adjacent buildings may substantially modify the interactions between water bodies and riparian vegetation.

These blue–green interactions are further conditioned by urban morphology, making their thermal effects highly context-dependent. Corridor orientation determines patterns of solar exposure, while alignment with prevailing winds influences the transport of cooled air from water surfaces into adjacent pedestrian spaces [32–34]. Likewise, wider waterways generally provide greater evaporative surfaces than narrow canals, although reported cooling effects vary considerably with local urban morphology [35–37]. Jiang et al. [38] identified that for green corridors along urban streams or creeks, a width of at least 20 m is required to effectively create an urban cool island. Empirical studies in the UK report cooling of approximately 0.3–1.6 °C within 100 m of canals during hot weather, but the magnitude of cooling remains highly site-specific [39,40]. These observations suggest that the effectiveness of blue–green infrastructure cannot be separated from surrounding urban form.

Regarding the planning and design of canal-edge walkways, several cities have developed relevant precedents. A notable example is New York's Waterfront Edge Design

Guidelines (WEDG), which provide standards for accessible and resilient waterfronts, with a focus on flood resilience, public access, and ecological performance [41]. Similarly, recent guidance on nature-based urban cooling advocates the integration of trees and water within urban design and planning [42,43]. While these policy and design frameworks promote blue–green infrastructure and support resilient waterfront development, they provide limited thermally oriented guidance for towpaths and linear canal-edge pedestrian corridors.

Above all, two critical gaps remain in particular. Firstly, empirical research on thermal environments and comfort in waterfront settings has predominantly focused on large water bodies, such as lakes, with comparatively limited attention given to hard-edged, narrow, linear canal corridors in urban environments, particularly in temperate climates such as the UK. Previous studies have primarily evaluated the cooling effects of individual blue or green elements, whereas the mechanisms governing their interactions within canal-edge environments remain poorly understood. Consequently, it remains unclear for canals which design factors ultimately control pedestrian thermal comfort and how these factors interact under heatwave conditions.

To address these knowledge gaps, this study aims to investigate how canal morphology, canal water and riparian vegetation interact to influence pedestrian thermal comfort along urban canal-edge walkways under heatwave conditions. Using Manchester city centre as a representative case study, a validated ENVI-met model and a parametric scenario matrix were employed to quantify both the individual and combined effects of canal orientation, canal width, water bodies and tree canopy configuration.

Accordingly, the study is guided by three research questions:

(1) How do canal orientation and canal width influence the baseline thermal environment of canal-edge walkways?
(2) What are the individual and synergistic contributions of canal water and riparian vegetation to pedestrian thermal comfort?
(3) How should riparian tree canopy configuration be optimised to maximise thermal comfort under different canal morphologies?

By addressing these questions, this study provides quantitative evidence on how canal morphology, water bodies and riparian vegetation jointly influence pedestrian thermal comfort in canal-edge environments. The findings contribute to climate-responsive canal-edge design while improving understanding of the interactions among blue–green infrastructure and urban morphology under extreme summer conditions. Although based on Manchester, the mechanistic insights and parametric relationships identified are intended to be transferable to similar canal-edge settings in temperate cities.

2. Materials and Methods

2.1. Study Area

The study area is in Manchester, in north-west England (53.48° N, 2.22° W). As a mid-latitude city with a temperate maritime climate (Köppen–Geiger classification: Cfb; [44,45]) and prevailing westerly to south-westerly winds, Manchester typically experiences mild summers, with average daytime temperatures around 20 °C [46]. However, extreme heat events have become more frequent in recent years, with air temperatures occasionally exceeding 30 °C. During the 2022 heatwave, unprecedented warnings were issued by the Met Office and the UK Health Security Agency, accompanied by record-breaking temperatures (37.2 °C) [47] and documented heat-related impacts [48].

This study focuses on the city centre of Manchester, a post-industrial urban area characterised by an extensive canal network [49]. The selected study area includes the Rochdale Canal, Bridgewater Canal, Castlefield Basin, and the New Islington area. Along these corridors, canal edges collectively form a continuous, multipurpose walking route that supports both mobility and recreation [50] (Figure 1).

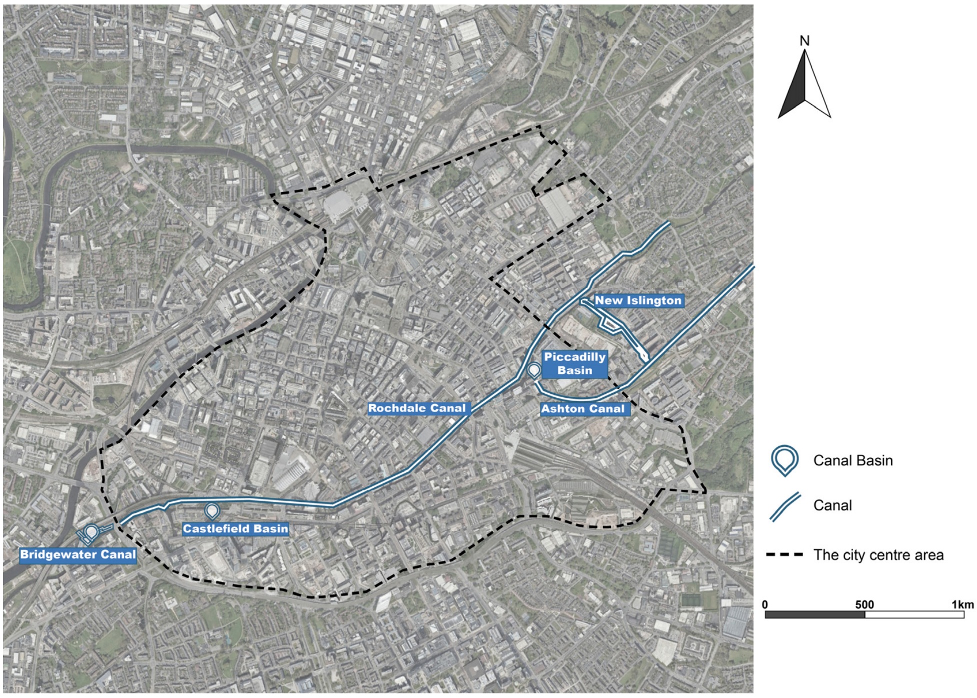

Figure 1. The Manchester city centre area comprising the wards of Deansgate and Piccadilly, and six typical canal sections. Source: Adapted from Google Earth imagery (captured 15 August 2025).

2.2. ENVI-Met Descriptions

ENVI-met (V5.6.1) was used as the primary simulation tool. It is a three-dimensional microclimate model widely applied in urban climate and outdoor thermal comfort studies [51]. The model couples wind flow, heat and radiation with plant/soil processes such as transpiration, with the capacity to resolve microscale interactions between buildings, vegetation and air [52]. Its performance has been validated for key variables such as air temperature and mean radiant temperature in multiple studies [53,54].

2.3. ENVI-Met Validation

Field measurements were conducted to validate the ENVI-met model using site-specific geographical and urban climate information [55]. The fieldwork took place on a clear summer day (13 August 2025) near the New Islington Canal, representing typical warm-weather conditions. Microclimate monitoring was carried out at two representative locations within the canal corridor, selected to capture contrasting thermal conditions: (1) a shaded spot beneath a mature *Salix alba* (white willow) with an estimated canopy spread of approximately 7 m, adjacent to the water, representing combined shading and evaporative cooling effects; and (2) an open, unshaded pavement surface composed of pre-grooved timber decking infilled with quartz-sand aggregate, representing high solar exposure conditions (Figure 2).

Measurements were obtained using two Kestrel 5400 weather trackers at a height of approximately 1.5 m for the microclimate condition at the pedestrian level. Data were recorded at 1 min intervals, capturing air temperature, globe temperature, relative humidity, and wind speed. Continuous observations were conducted over an 8 h daytime period (9:00–17:00 BST) to capture both peak heating and the onset of cooling, following the established microclimate field measurement guidelines [56].

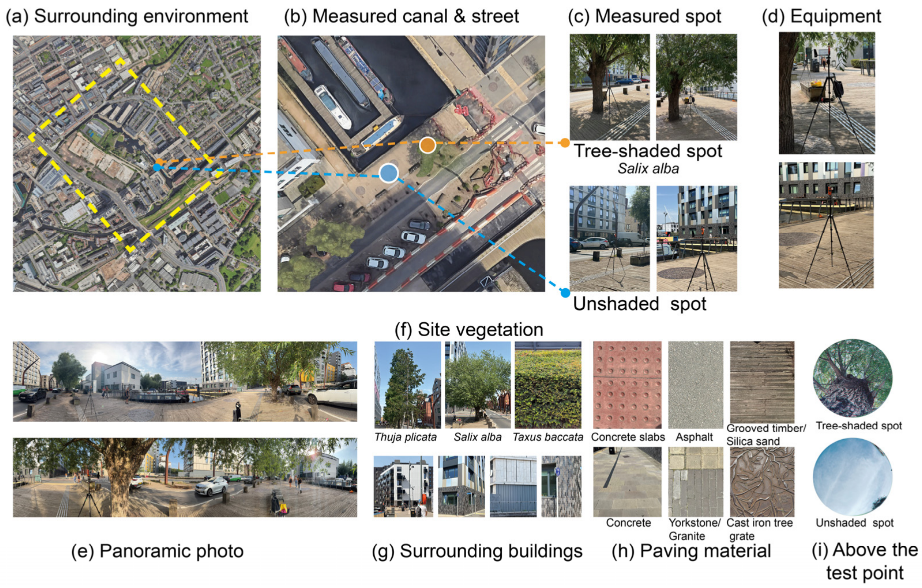

Figure 2. Field measurement setup near the New Islington Canal, showing the tree-shaded (53.48° N, 2.22° W) and unshaded (53.48° N, 2.22° W) sites.

The ENVI-met model was initialised using observed meteorological conditions, with vegetation parameters adjusted to reflect site-specific characteristics. Model outputs were extracted from grid cells corresponding to the measurement locations (Figure 3). These outputs were compared with field observations using a centred ±30 min averaging window at each full hour, a common approach to reduce temporal representativeness error and align with "hour-ending" reporting conventions [57,58]. Model performance was evaluated using standard statistical metrics, including the coefficient of determination (R^2), root mean square error (RMSE), mean absolute error (MAE), and mean bias error (MBE). MAE complements RMSE as a robust indicator of average error magnitude [59]. The definition of these metrics can be found in Willmott [60] and Stunder and Sethuraman [61]. The final ENVI-met configuration based on the field site is shown in Figure 3.

Figure 3. ENVI-met model of the validation area near the New Islington canal.

2.4. Simulation Setup

2.4.1. Meteorological Conditions

To represent the extreme summer condition in Manchester, the heatwave event on 19 July 2022 was selected in parametric simulations, during which Greater Manchester recorded peak air temperatures of up to 38 °C [47]. Hourly meteorological data, including air temperature, relative humidity, and wind speed and direction, were obtained for this day and used as boundary and initial conditions for the Simple Forcing simulation (Appendix A). This period captures the main daytime heating phase, with air temperature increasing from 31.11 °C at 08:50 to a recorded maximum of 37.78 °C at 14:20, before gradually declining during the late afternoon. Relative humidity decreased from 29% in the morning to around 20% during the hottest period, while wind speed increased through the afternoon [62]. The selection of a heatwave day in simulation is consistent with previous ENVI-met studies, which commonly use the hottest day or heatwave scenarios to observe the microclimatic effects of trees, water bodies and urban-surface configurations [51,63].

The ENVI-met simulations were initialised at 9:00 and run for eight hours, ending at 17:00. Clear-sky conditions were applied across all scenarios to maintain consistent solar-radiation forcing.

2.4.2. Generic Canal Model Development

A generic model was developed based on typical canal-edge morphology in areas such as Castlefield, Ancoats, and New Islington in Manchester. These locations are characterised by linear canal networks, mid-rise building forms, and refurbished pedestrian-oriented public spaces, making them representative of common canal-side urban morphologies across the study area, including the common dimensions, styles, water width and vegetation conditions of adjacent footpaths (Figure 1) [64,65]. This abstraction enables controlled testing of microclimatic responses to design interventions while retaining key morphological characteristics of real canal corridors.

The canal-side walkway was parameterised as a 6 m wide corridor on each bank. Of this, 3 m was allocated to a shared pedestrian–cycle path, with the remaining width reserved for a narrow green verge and setback buffer to accommodate maintenance access and safe passing. This configuration aligns with Canal & River Trust towpath guidance, which recommends multi-user routes of about 2 m within wider towpath corridors and encourages greater widths where feasible. This also aligns with UK active travel standards, which recommend widths of around 3 m for well-used shared paths [66,67]. Buildings along both canal banks were simplified as uniform rectangular blocks with a nominal height of 20 m (approximately 6–7 storeys) and a depth of 15 m, with predominantly brick and masonry façades. These parameters reflect the prevailing mid-rise, brick-dominated urban fabric in areas such as Ancoats and Castlefield, where historic mill and warehouse typologies define the canal frontage [68,69].

The model dimensions were 100 m on one side, while the other side containing the canal was 50 m or 62 m, depending on whether the canal width was 8 m or 20 m (rationale explained in Section 2.4.3), respectively. The model's horizontal resolution was 1 m. To account for variability in solar exposure and ventilation, two canal orientations (north–south and east–west) were included in the simulation matrix to represent contrasting airflow conditions [70–72]. Together, these parameters define the baseline conditions for subsequent planting and design scenario testing. The ENVI-met model configuration is shown in Figure 4.

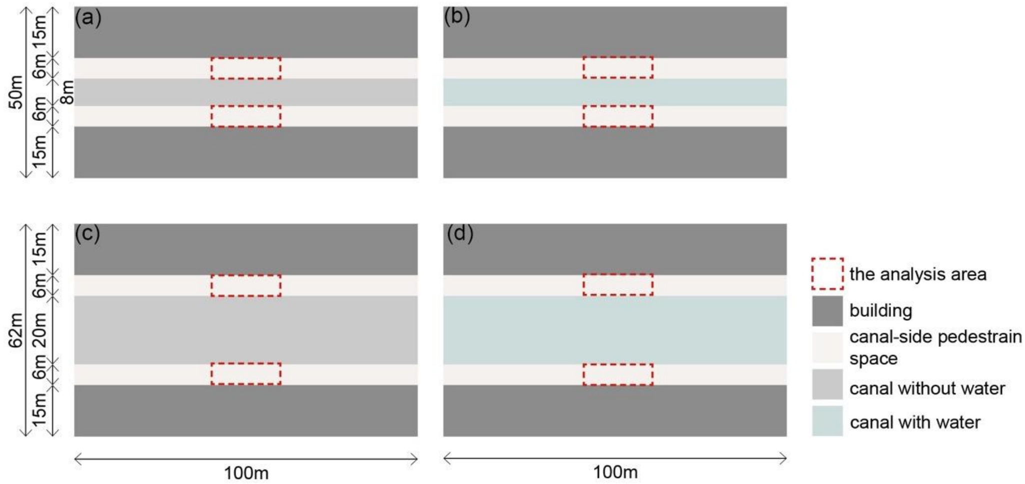

Figure 4. The generic models with different canal widths (taking canals with E–W orientation as examples). (**a**,**c**): Reference models with different canal widths (canals without water); (**b**,**d**): Canals with different widths.

2.4.3. Scenario Development

Following the establishment of the generic model, a series of parametric simulation scenarios were developed to investigate the combined effects of canal morphology and tree planting design on microclimate and human thermal comfort performance (Table 1).

Table 1. Thermal conditions in the four baseline scenarios (without any blue-green element interventions).

Canal Orientation		**N–S**		**E–W**	
Canal Width		**8 m**	**20 m**	**8 m**	**20 m**
Microclimate and outdoor human thermal comfort conditions	**TA (°C)**	37.08	37.27	37.00	37.35
	RH (%)	21.11	20.92	21.46	21.11
	MRT (°C)	58.98	60.70	63.84	61.63
	WS (m/s)	1.75	1.75	0.75	0.75
	PET (°C)	49.08	48.12	50.35	49.14

Canal Morphology

A set of baseline scenarios (reference scenarios) was first constructed, representing the urban background conditions without blue-green infrastructure interventions. These scenarios included only the built environment (i.e., buildings, hard surfaces, and canal-side walkways) and were defined by two key variables: canal orientation and width. Two orientations (N–S and E–W) were incorporated to investigate the thermal effect from solar exposure and building-induced shading. To assess the cooling effect of water, canal sections were alternatively modelled as either water bodies or hard-surfaced areas without water (Figure 4).

To ensure realistic representation of canal morphology in Manchester, two representative canal widths were defined based on field observations, case studies, and UK waterway design guidance [50,73,74]. Six canal samples in Manchester city centre (Figure 1) were analysed to summarise the usual width and orientation (Appendix B). A "narrow" canal width of 8 m was adopted to reflect typical historic canals in Manchester (e.g., the Ashton Canal), where constrained geometries remain common. Although lock dimensions are narrower, design guidance generally indicates wider surface conditions; thus, 8 m represents a conservative but realistic urban water width [75,76]. A "wide" canal scenario of 20 m was introduced as a representative parametric condition for broader urban canal sections and canal basins within Manchester's wider waterway network, which includes the Manchester Ship Canal [77]. This study focuses on engineered urban canals with hard-edged boundaries (e.g., quays, towpaths, and adjacent buildings), which form well-defined urban canyon geometries. Natural rivers, typically characterised by more extensive vegetation and different hydraulic and ecological processes, were excluded from the scope [78].

Tree Planting Design

(1) Tree planting intervals

Two tree planting intervals, 5 m and 10 m, were tested to represent relatively dense and open street-tree configurations within a realistic UK design range. Typical guidance suggests spacings of approximately 8–12 m [79], while closer planting (approximately 5 m) may be appropriate for medium-sized or fastigiate species where space is constrained [80]. These values are consistent with observations from Manchester, where street trees are commonly spaced at 7–10 m [81]. Accordingly, ENVI-met scenarios were defined using 5 m and 10 m intervals (Figure 5).

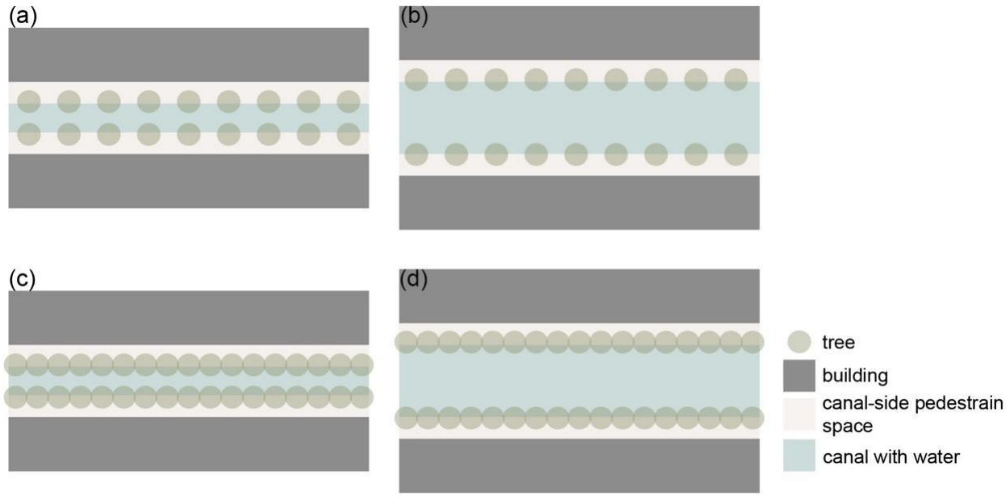

Figure 5. Schematic illustrations of the ENVI-met models for tree planting intervals (taking canals with E–W orientation as examples): (**a**) scenarios with 8 m canal width and 10 m tree planting intervals; (**b**) scenarios with 20 m canal width and 10 m tree planting intervals; (**c**) scenarios with 8 m canal width and 5 m tree planting intervals; (**d**) scenarios with 20 m canal width and 5 m tree planting intervals.

(2) Tree crown density

Leaf area index (LAI) was used to represent tree crown density. Three LAI values (1.5, 3, and 5) were selected to represent low, medium, and high canopy conditions. Empirical evidence from Manchester, UK, together with recent urban-tree LAI measurements, indicates that deciduous street trees commonly fall within an LAI range of approximately 2–4, while values rarely exceed 5 even for dense canopies [81,82]. One reason for this is that street trees are often planted in small pits, which restrict the growth of their canopies. This is also the case in Manchester. These three levels of LAI therefore capture a realistic range from sparse to dense urban canopy conditions.

To link LAI values to representative tree species, three common street tree species in Manchester were selected from the ENVI-met tree library (Figure 6). This study did not adjust LAI by simply varying the size of a single tree species model. Instead, variations in LAI were represented by using different tree species. This approach was primarily adopted to better reflect the real-world conditions of street trees in Manchester, allowing us to capture and analyse the morphological differences among trees in practice. Here, *Tilia × europaea* was used to represent the high-LAI scenario, as common lime is comparable to small-leaved lime and has an LAI close to the dense-canopy condition reported in recent urban-tree measurements [82]. *Betula pendula* (silver birch) was used for the medium-LAI scenario, given its prevalence in Greater Manchester and its reported LAI of approximately 3 [82–84]. *Sorbus arnoldiana* (rowan) represented the low-LAI scenario, with an LAI of approximately 1.5 [81].

For modelling consistency, trees were generalised as small-to-medium and medium-sized street trees with mature heights of approximately 10–17 m and crown spreads of 6–11 m, following UK urban tree guidance that emphasises selecting tree size according to site constraints and designing for the largest long-lived species suitable for the available space [85–87]. In constrained canal-side spaces, columnar or fastigiate tree forms were assumed to be necessary to reduce conflicts with buildings and pedestrian movement, consistent with UK street-tree guidance for constrained urban settings [87,88]. A medium canopy diameter of approximately 5 m was adopted as a representative condition for urban streetscapes, consistent with hard-landscape tree-pit assumptions for medium-sized trees such as *Betula pendula* [89].

Combining these tree planning designs with water and canal morphology, a total of 32 scenarios were simulated (Appendix C). These scenarios can be classified into three categories: reference scenarios without any landscape intervention, scenarios with only water bodies, and scenarios incorporating both green and blue elements. This full-factorial design enables systematic evaluation of both individual parameter effects and their interactions. All boundary conditions and simulation durations were held constant to ensure that differences in outcomes can be attributed solely to the tested variables.

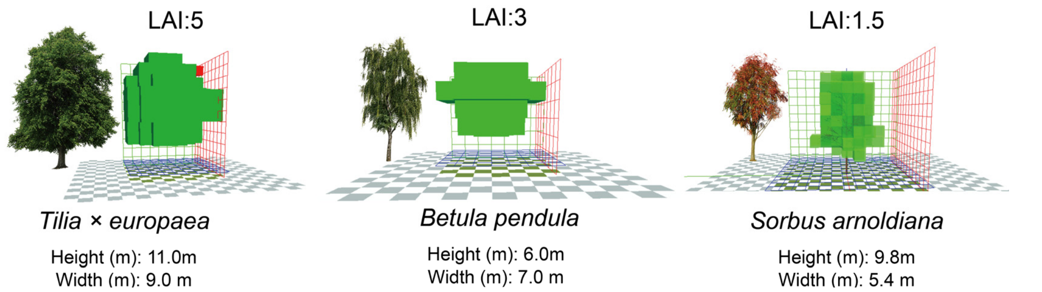

Figure 6. The ENVI-met tree models and their representative real-tree photographs. Source: Pépinières Thuilleaux [90], Keele University [91] and Plant Photo Bank of China (PPBC) [92]. Green blocks represent the ENVI-met tree grid cells.

2.5. Data Analysis

2.5.1. Data Collation

For each scenario, four microclimatic variables were extracted from ENVI-met at 1.5 m above ground level: air temperature (TA), relative humidity (RH), wind speed (WS), and mean radiant temperature (MRT). MRT represents the uniform radiant temperature of an enclosure that would produce the same net radiative exchange with the human body as the actual outdoor environment. By integrating both shortwave and longwave radiation, it is a key determinant of outdoor heat load [93,94].

Human thermal comfort was assessed using Physiological Equivalent Temperature (PET), estimated by BIO-met (an ENVI-met module). Expressed in °C, PET integrates TA, RH, WS, and MRT, while accounting for clothing insulation and activity level, making it a widely used index for evaluating outdoor thermal comfort at pedestrian level [95,96]. This allows both physical and perceived thermal conditions to be evaluated in an integrated manner. The PET thresholds were referenced from those established for Central Europe [96].

Simulation outputs at 3 p.m. were selected for scenario comparison because it represents the period of maximum pedestrian thermal stress within the simulation window [63], when thermal conditions typically reach their daily maxima under clear summer conditions in built environments [93,97].

2.5.2. Statistical Methods

The analysis focuses on the canal-side pedestrian space between the canal and the adjacent buildings. To minimise boundary effects and improve the reliability of simulation results, all statistics were calculated within a central analysis zone (Figure 4), set back from the lateral edges in accordance with ENVI-met guidance on buffer and nesting areas [98]. Within this zone, spatial mean values of TA, RH, WS, MRT, and PET at a pedestrian height were computed across the canal-side walkway. This approach represents the typical thermal experience along the canal rather than conditions at isolated points. In street canyons, radiation and shading vary sharply over short distances; therefore, single-point maxima are highly sensitive to transient sun patches and may not reflect overall conditions. Using spatial averages reduces local variability, improves comparability across different canal orientations, canal widths, and planting configurations, and aligns with planning-oriented approaches that assess outdoor comfort at the area scale [93,99].

3. Results

3.1. Model Validation

In the validation, the regression trends exhibited strong linear relationships between simulated and measured values (Figure 7), suggesting that the ENVI-met model adequately reproduced both the magnitude and temporal variability of the observed microclimatic conditions. The simulated results showed good agreement with field measurements for both TA and RH (Appendix D). TA was simulated with high accuracy, particularly at the tree-shaded site (R^2 = 0.99, RMSE = 0.50 °C), while acceptable performance was also achieved in the unshaded area (R^2 = 0.85, RMSE = 1.11 °C). RH simulations were reasonably consistent with observations, with R^2 values of 0.86 and 0.91 for the tree-shaded and unshaded sites, respectively (Appendix D). Although the model slightly overestimated RH beneath the canopy (MBE = +1.51%), overall errors remained low. These results indicate that the model adequately reproduced the observed microclimatic conditions and is suitable for subsequent simulations.

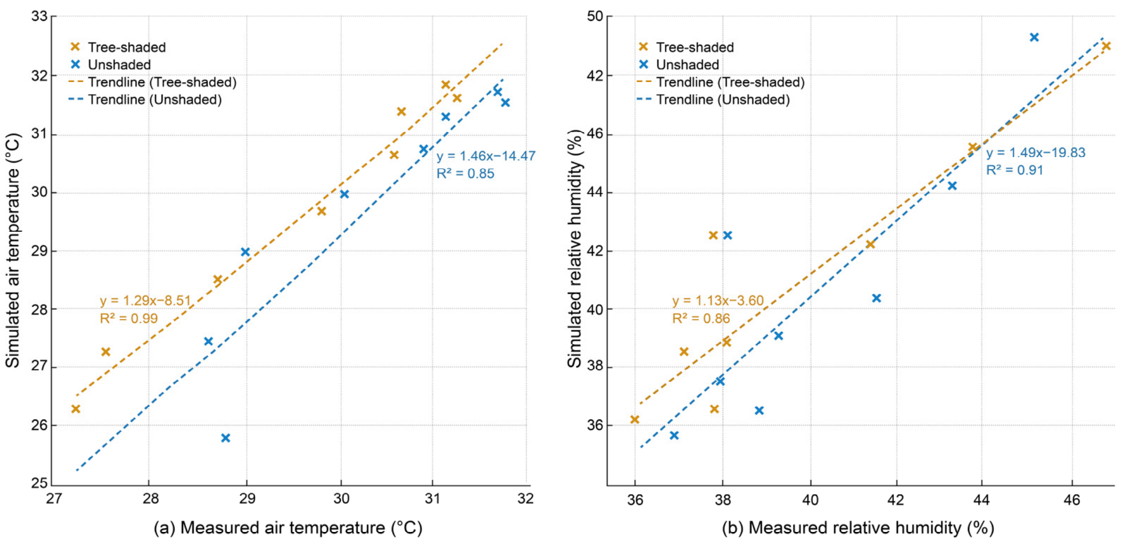

Figure 7. Relationship between simulated and field-measured (**a**) air temperature and (**b**) relative humidity at tree-shaded and nearby unshaded areas.

3.2. The Thermal Effects of Canal Morphology

The thermal conditions of the four baseline scenarios at 3 p.m. are presented in Table 1. The scenarios without blue–green interventions were used to evaluate the influence of canal morphology (orientation and width) on the microclimate of adjacent pedestrian spaces. During the hottest period of the day, all baseline scenarios experienced very hot thermal conditions and extreme heat stress [96]. Among them, the E–W-oriented canal with a width of 8 m exhibited the poorest thermal environment, with the highest PET (50.35 °C) and MRT (63.84 °C), indicating the greatest pedestrian heat exposure.

Canal orientation exerted a stronger influence on thermal conditions than canal width. Across both canal widths, E–W-oriented canals consistently exhibited higher MRT and PET than N–S-oriented canals. At the 8 m width, the E–W orientation increased MRT and PET by 4.86 °C and 1.27 °C, respectively, relative to the N–S orientation. Similar but smaller differences were observed for the 20 m canal, where MRT and PET were 0.93 °C and 1.02 °C higher, respectively. By comparison, differences in air temperature were small across all scenarios (≤0.35 °C), while wind speed remained identical within the same canal orientation.

The influence of canal width was comparatively limited. The 20 m canal consistently showed slightly higher air temperatures than the 8 m canal, with differences of 0.19 °C for the N–S orientation and 0.35 °C for the E–W orientation. However, no consistent trend was observed for MRT or PET. Under the N–S orientation, the wider canal exhibited slightly lower MRT and PET, whereas the opposite pattern occurred under the E–W orientation.

3.3. The Cooling Effect of Water Bodies

To evaluate the cooling effect of canal water, the four water-only scenarios were compared with their corresponding baseline scenarios (Table 2). Introducing water bodies improved the outdoor thermal environment across all canal configurations, with PET reductions ranging from 1.33 to 2.58 °C. Nevertheless, these improvements were insufficient to produce a substantial change in thermal perception, as PET values remained within the "very hot" category.

Table 2. Comparison of thermal conditions between the four scenarios incorporating only water bodies and their corresponding baseline scenarios (Note: ΔTA = TA of the baseline scenario − TA of the water-body scenario; the same calculation applies to the other variables).

Canal Orientation		**N–S**		**E–W**	
Canal Width		**8 m**	**20 m**	**8 m**	**20 m**
Microclimate and outdoor human thermal comfort conditions	**ΔTA (°C)**	1.35	1.86	1.01	2.13
	ΔRH (%)	−2.65	−3.41	−1.66	−3.69
	ΔMRT (°C)	3.33	4.34	2.54	4.02
	ΔWS (m/s)	0.01	0.00	0.01	0.02
	ΔPET (°C)	2.3	2.33	1.33	2.58

The magnitude of cooling varied with canal morphology. Among all scenarios, the 20 m-wide E–W-oriented canal exhibited the greatest cooling response following water introduction, with reductions of 2.13 °C in TA, 4.02 °C in MRT and 2.58 °C in PET, together with the largest increase in RH (3.69%). Overall, the 20 m canal consistently produced larger reductions in TA, MRT and PET, as well as greater increases in RH, than the corresponding 8 m canal, regardless of orientation.

Canal orientation also influenced the effectiveness of water cooling. Within the 8 m canal scenarios, the E–W-oriented canal showed comparatively smaller reductions in PET, MRT, TA and RH than the N–S-oriented canal, indicating that the thermal benefit provided by canal water varied according to the surrounding canal morphology.

3.4. Synergistic Effects of Riparian Trees and Water Bodies

3.4.1. Synergistic Cooling Effect of Blue–Green Elements

Table 3 presents the thermal conditions of the E–W-oriented canal scenarios with LAI 5 trees planted at 5 m intervals, illustrating the synergistic cooling effects of combined blue–green infrastructure. Regardless of canal width, scenarios incorporating both canal water and riparian trees consistently produced better microclimatic conditions and outdoor thermal comfort than either the baseline or water-only scenarios.

Table 3. Comparison of thermal conditions between the scenario with waterfront trees and the corresponding scenario without trees (using the E–W canal scenario with the introduction of *Tilia × europaea* tree (LAI 5) planted at 5 m intervals as an example).

Canal Orientation		E–W					
Canal Width		**8 m**			**20 m**		
Water introduction condition		✓	✓	-	✓	✓	-
Tree planting condition		✓	-	-	✓	-	-
Microclimate and outdoor human thermal comfort conditions	**TA (°C)**	33.05	35.99	37.00	32.73	35.22	37.35
	RH (%)	28.08	23.12	21.46	29.38	24.8	31.11
	MRT (°C)	27.74	61.30	63.84	28.29	57.61	61.63
	WS (m/s)	0.64	0.74	0.75	0.65	0.73	0.75
	PET (°C)	32.45	49.02	50.35	32.22	46.56	49.14

The combined intervention substantially reduced pedestrian heat stress. Thermal perception improved from “very hot” to “warm”, while heat stress was reduced from “extreme” to “moderate”. PET reductions ranged from 14.35 to 17.90 °C, demonstrating that the introduction of trees contributed considerably greater cooling than water alone.

Similar improvements were observed for the microclimatic variables. Compared with the corresponding water-only scenarios, the addition of trees further reduced MRT by 33.56 °C and 29.32 °C for the 8 m and 20 m canals, respectively. Air temperature decreased by a further 2.94 °C (8 m) and 2.49 °C (20 m), while relative humidity increased by 4.96% and 4.58%, respectively. By contrast, tree planting produced only slight reductions in wind speed (0.10 m/s and 0.08 m/s), indicating that the substantial improvements in thermal comfort were achieved without major changes in local airflow.

3.4.2. The Cooling Effects Among Various Planting Methods for Waterside Trees

Evaluate the Integrated Cooling Effect of Tree Planting Configuration

Figure 8 presents the overall cooling performance of different tree planting configurations under varying canal morphologies. The introduction of riparian trees consistently improved the thermal environment across all scenarios, regardless of canal orientation, canal width or planting configuration. Reductions in PET closely corresponded with reductions in air temperature, indicating that improved microclimatic conditions were consistently accompanied by enhanced pedestrian thermal comfort.

Cooling performance differed substantially among planting configurations. Across all canal morphologies, the greatest reductions in PET and TA were consistently achieved by scenarios combining LAI 5 with a 5 m planting interval, while the weakest performance occurred under the LAI 1.5 scenarios with a 10 m interval. The maximum cooling effect was observed in the E–W-oriented 8 m canal, where PET decreased from approximately 49 °C to 32 °C, corresponding to a maximum reduction of 16.60 °C. By comparison, the E–W-oriented 20 m canal produced the second-largest PET reductions (13.9–14.3 °C), whereas all N–S-oriented canals showed comparatively smaller but still substantial improvements.

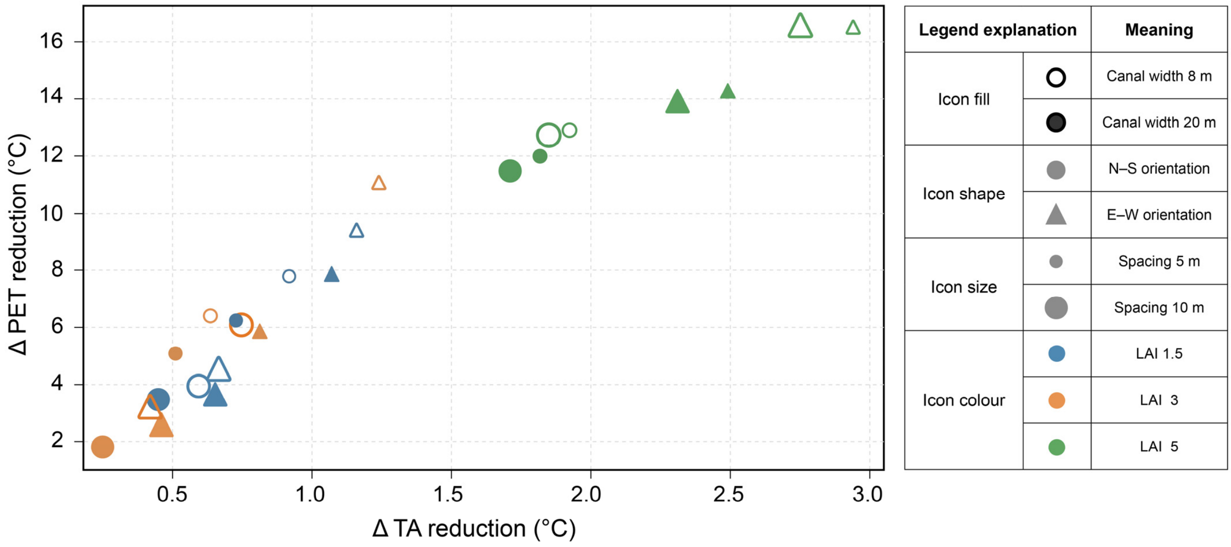

Figure 8. Comparing the cooling effects of tree planting configurations in different scenarios. (Note: TA reduction = TA of the water-body scenario − TA of the waterside tree planting scenario; the same calculation applies to ΔPET).

Overall, Figure 8 demonstrates that the cooling response differed markedly across LAI levels. Increasing LAI from 3 to 5 produced considerably greater reductions in TA and PET than increasing LAI from 1.5 to 3, with the magnitude of these reductions varying across canal morphologies, planting intervals and canopy density. The respective influences of these factors are examined in the following analyses.

Cooling Effects of Planting Interval

Figure 9 compares the influence of tree planting interval on the cooling performance of canal-edge blue–green infrastructure. Across almost all scenarios, reducing the planting interval from 10 m to 5 m enhanced thermal performance, although the magnitude of improvement varied with canopy density and canal morphology.

The influence of planting interval was most evident for PET. Under the 5 m interval, PET reductions ranged from 2.45 to 16.60 °C, compared with 1.82–14.30 °C under the 10 m interval. The benefit of closer spacing became increasingly apparent under denser canopies, whereas differences between planting intervals were relatively small for sparse canopies.

Similar trends were observed for TA and MRT. Air-temperature reductions ranged from 0.51 to 2.94 °C under the 5 m interval compared with 0.25–0.75 °C under the 10 m interval (with only one exception occurring in the N–S-oriented 8 m canal with LAI 3, where the wider spacing produced slightly greater cooling). MRT reductions ranged from 14.57 to 33.56 °C under the 5 m interval and 7.68–33.26 °C under the 10 m interval. Across all canal morphologies, the closer planting interval consistently generated larger MRT reductions, with differences ranging from 0.30 to 15.09 °C. Overall, decreasing planting interval generally strengthened the cooling performance of canal-edge trees, particularly where canopy density was sufficiently high.

Cooling Effects of Tree Crown Density

Overall, increasing canopy density generally enhanced the cooling performance of canal-edge blue–green infrastructure (Figure 9), although the relationship was not strictly linear across all scenarios. Trees with LAI 5 consistently produced the greatest reductions in PET, TA and MRT, irrespective of canal morphology or planting interval. However, increasing canopy density from LAI 1.5 to LAI 3 did not always improve cooling performance. For example, under the 20 m-wide canal with a 10 m planting interval, PET reduction decreased from 3.46 °C to 1.82 °C in the N–S orientation and from 3.65 °C to 2.59 °C in the E–W orientation when LAI increased from 1.5 to 3. By contrast, increasing canopy density from LAI 3 to LAI 5 produced substantial improvements across all canal morphologies. Additional PET reductions ranged from 5.41 to 13.41 °C, with the greatest improvement observed in the E–W-oriented 8 m canal with a 10 m planting interval. Similar patterns were observed for TA and MRT, where trees with LAI 5 consistently achieved the largest reductions regardless of planting interval. These results indicate that higher canopy density generally provides greater cooling benefits, although increases in cooling performance do not occur proportionally with increasing LAI.

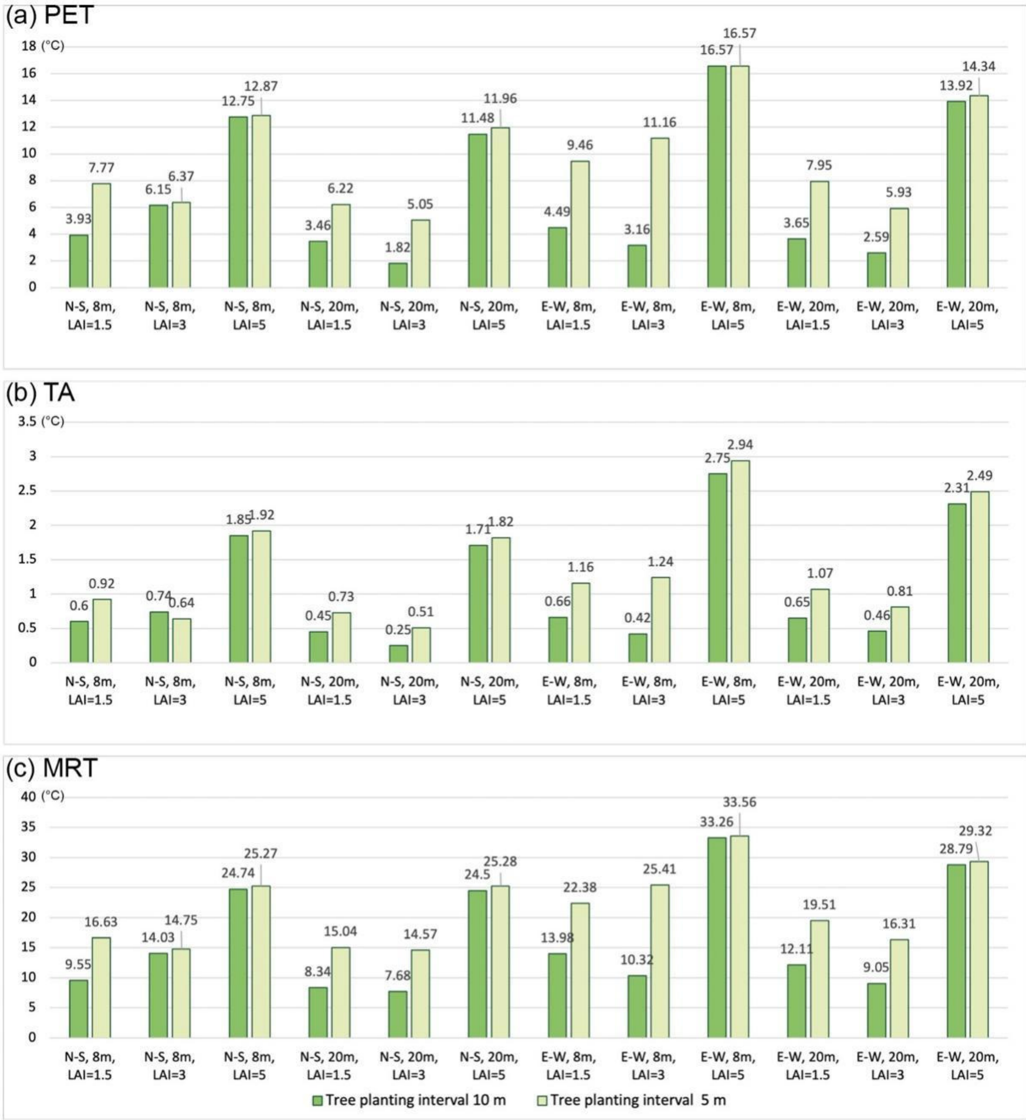

Figure 9. Effects of different tree planting intervals on improvements in thermal environment and human thermal comfort (**a**) PET reduction (**b**) TA reduction (**c**) MRT reduction (Note: PET reduction = PET of the scenario with waterbodies only − PET of the scenario with both blue and green elements; the same calculation applies to TA and MRT reduction).

4. Discussion

4.1. The Role of Canal Orientation in Shaping Fundamental Thermal Conditions

The baseline scenarios indicate that, in the absence of blue-green interventions, the E–W-oriented canal-edge walkway produced less favourable pedestrian-level thermal conditions in the summer afternoon, which could be attributed to stronger direct solar exposure on the walkway surface and adjacent building façades, resulting in a higher absorbed direct and reflected solar and terrestrial radiation by the human body. By contrast, the N–S-oriented walkway showed a lower level of pedestrian heat stress. This is consistent with the findings of multiple street-canyon-related studies, showing that E–W streets concentrate solar exposure and lead to worse thermal comfort than the other orientations and it is difficult to optimise by varying canyon aspect ratios [100,101]. In this regard, this phenomenon has been comprehensively explained by Shashua-Bar and Hoffman [102]: the intensity of solar radiation reaching the street surface depends on both the street axis azimuth and the solar azimuth. Although the total daily incident solar radiation received by the street's ground surface may not differ substantially, clear differences can emerge at specific times of the day (e.g., 3 p.m.).

In addition to radiation, the simulated wind field further helps explain the observed orientation effect. Under the southerly prevailing wind direction, the N–S-oriented canals were aligned with the incoming airflow and showed a higher mean pedestrian-level wind speed of 1.75 m/s. In contrast, the E–W-oriented canals were more sheltered from buildings, with a lower mean wind speed of 0.75 m/s. This ventilation difference reduced convective heat exchange in the E–W-oriented canals.

4.2. The Contribution of Canal Water to Pedestrian Thermal Comfort

The results in Section 3.3 show that introducing water bodies can improve the thermal environment of canal-edge pedestrian spaces to some extent, but the improvement magnitude was moderate and strongly dependent on canal orientation and local ventilation conditions. The magnitude of the simulated TA reduction (1.01–2.13 °C) is comparable with other canal-cooling studies in the UK, which reported that canals can reduce local summer temperatures by more than 1 °C during hot weather conditions [39,103]. However, canal water can provide measurable daytime cooling during heatwave conditions, but introducing water alone was not sufficient to fundamentally change the level of outdoor thermal comfort and heat stress in the summer afternoon, as compared with the corresponding no-water baseline scenarios, as the four water-introduced scenarios reduced PET only by 1.33–2.58 °C. This is supported by Jacobs et al. [36] who stated that small water bodies have only a limited local cooling effect at the pedestrian level, making their impact in practical design applications almost negligible. However, it should also be emphasized that the conclusion reported by Jacobs et al. was derived under different climatic conditions. Their relatively modest simulated cooling effects (with an average cooling effect of 0.2 °C and maximum cooling effect of 0.6 °C) were largely attributable to the Dutch climate scenario adopted, which assumed a daily maximum TA of approximately 30 °C and middle cloud conditions. By contrast, this study simulated a much hotter environment, with daily maximum TA reaching approximately 38 °C under clear-sky conditions. In fact, the influence of water bodies on the urban thermal environment is also related to multiple factors, including water depth, waterbody geometry, embankment height, surrounding urban spatial morphology, background climatic conditions, and time of day [31,36,104]. The heat and mass transfer processes involved are highly complex, and the magnitude of these effects still requires further quantitative investigation [105]. In addition, Teshnehdel et al. [106] suggested that although evaporation from open water bodies without tree cover can reduce air temperature, it may simultaneously increase ambient humidity, thereby diminishing its positive effect on thermal comfort. However, considering that the UK is expected to experience drier summers under future climate change [107], an increase in humidity may instead have a beneficial effect on the thermal environment in the UK context.

The 20 m canal produced greater reductions in TA and MRT and increases in RH than the 8 m canal (Section 3.3). However, the thermal-comfort benefit associated with wider water surfaces did not increase uniformly across orientations (for the E–W orientation, widening the canal from 8 m to 20 m substantially increased PET reduction, from 1.33 °C to 2.58 °C while for the N–S orientation, the corresponding PET reduction increased only marginally, from 2.30 °C to 2.33 °C). Therefore, wider canals should not be simply interpreted as thermally more comfortable under all conditions; the extent to which this improved pedestrian thermal comfort depended on the surrounding urban context, especially radiation and ventilation conditions. Canal widening is most effective where airflow can transport cooled air from the water surface toward the pedestrian zone; where ventilation is weak, increasing width alone may provide limited comfort benefit [31,108]. Therefore, the primary design value of canal water may lie less in its direct cooling effect than in its capacity to enhance the performance of adjacent riparian vegetation, which is discussed in Section 4.3.

4.3. Understanding Green–Blue Interactions in Canal-Edge Cooling

The results presented in Section 3.4 demonstrate that introducing riparian trees substantially enhanced the cooling performance of canal-edge spaces compared with both the baseline and water-only scenarios. Although canal water alone produced measurable reductions in pedestrian heat stress, its cooling effect remained relatively modest during summer afternoons. By contrast, when combined with riparian trees, the thermal environment improved considerably, particularly in terms of MRT and PET. These findings suggest that the cooling performance of canal-edge environments reflects the combined influence of blue and green infrastructure, with canopy shading emerging as the dominant mechanism. Rather than functioning as the dominant cooling source itself, canal water appears to play a supportive role by creating environmental conditions that enhance the cooling efficiency of adjacent vegetation.

The simulation results further indicate that the dominant mechanism underlying this synergistic effect is the reduction in radiant heat load through canopy shading rather than substantial decreases in air temperature. For example, under the E–W-oriented 20 m canal scenario planted with LAI 5 trees at 5 m intervals, MRT was 33.34 °C lower than in the baseline scenario and 29.32 °C lower than in the water-only scenario, whereas the corresponding reductions in air temperature were considerably smaller. Previous field and modelling studies have similarly reported substantial shading-related reductions in pedestrian thermal exposure, including globe-temperature reductions of approximately 5–7 °C in Manchester and pedestrian-level MRT reductions of up to 23 °C in street-canyon simulations [109,110]. Although these values are not directly comparable because of differences in climate, urban geometry and reference conditions, they support the dominant role of canopy shading identified in the present study. This disproportionate response indicates that pedestrian thermal comfort was improved primarily through reducing exposure to shortwave and longwave radiation rather than through modifying the surrounding air temperature. This interpretation is consistent with previous studies showing that mean radiant temperature is a key driver of daytime outdoor thermal comfort and that urban trees improve pedestrian-level conditions primarily through shading and reductions in radiant heat exposure. Collectively, these results support what this study terms a shade-dominant interpretation of canal-edge cooling, in which pedestrian thermal comfort is improved mainly through canopy-driven reductions in radiant heat load, consistent with previous work on tree shading and mean radiant temperature as a driver of outdoor thermal comfort [111].

This interpretation is consistent with the theoretical framework proposed by Tim Oke in *The Micrometeorology of the Urban Forest*. Owing to their morphological similarities to urban street canyons, canal-edge spaces receive substantial direct solar radiation together with reflected shortwave radiation and emitted longwave radiation from adjacent buildings and paved surfaces. Tree canopies intercept a large proportion of these radiative fluxes while dissipating absorbed energy through evapotranspiration and sensible heat exchange, thereby substantially reducing the radiant heat load experienced by pedestrians [112,113]. Similar conclusions have been reported by previous studies [27,114,115], which consistently demonstrate that combined green–blue configurations provide stronger daytime cooling than either vegetation or water alone, particularly where tree shade is the primary contributor to thermal comfort improvement [28].

In addition, canal water may indirectly support the cooling performance of adjacent riparian trees by modifying local atmospheric and soil-moisture conditions. Under Manchester's summer conditions, evaporation from the canal may slightly increase ambient humidity and reduce vapour pressure deficit [116], while proximity to the waterbody may also improve soil-water availability and reduce water stress in riparian trees [117]. These conditions may help sustain transpiration and tree cooling performance during hot periods. Although these physiological processes were not explicitly simulated in the present study, they provide a plausible explanation for the stronger cooling observed in the coupled blue-green scenarios and warrant further investigation. Furthermore, this mechanism may become increasingly important under future climate change, as hotter and drier summers are projected across the UK, making water availability an increasingly important constraint on urban vegetation cooling. In this regard, the long-term value of urban canals may extend beyond their direct evaporative cooling effect to supporting the resilience and cooling capacity of adjacent urban vegetation.

Nevertheless, the synergistic effect should not be regarded as universally positive. Dense riparian planting may reduce pedestrian-level ventilation and weaken convective heat removal, particularly within poorly ventilated canal-edge spaces. In the present study, although tree planting slightly reduced local wind speed, this effect did not offset the substantial cooling benefit generated by canopy shading, as PET continued to decrease markedly. The results therefore suggest that successful canal-edge design should not aim simply to maximise tree density or water area, but rather to optimise the balance between radiative shading, vegetation cooling, and pedestrian ventilation. The effectiveness of blue-green infrastructure should consequently be understood as a context-dependent interaction among radiation, airflow, and vegetation configuration rather than as a universally additive cooling strategy [118–120].

4.4. Tree Canopy Configuration as the Primary Determinant of Canal-Edge Thermal Performance

The findings suggest that the cooling performance of canal-edge trees is governed not by individual planting parameters in isolation, but by the overall canopy configuration, particularly its capacity to provide sufficiently continuous shading over pedestrian spaces. Across the tested scenarios, higher canopy density (represented by LAI) and closer planting intervals generally produced greater reductions in air temperature (TA), mean radiant temperature (MRT), and physiological equivalent temperature (PET) (Figure 8). However, the relationship between these planting parameters and cooling performance was not strictly linear, indicating that tree-induced cooling depends on complex interactions between canopy structure, spatial arrangement, and local microclimatic processes. In several cases, increasing LAI from 1.5 to 3 produced limited or even reduced thermal benefits, whereas increasing LAI from 3 to 5 generated substantially larger reductions in MRT, TA, and PET. This pattern indicates that cooling effectiveness may increase disproportionately once canopy structure reaches a critical threshold at which shading becomes sufficiently extensive and spatially continuous. Rather than leaf area itself, the key mechanism appears to be the extent to which additional foliage reduces direct solar exposure and minimizes sun gaps within pedestrian spaces. This interpretation supports the argument of Liu et al. [121] that, within a certain range, expanding the spatial extent of tree shade may contribute more effectively to outdoor thermal comfort improvement than simply increasing shade density.

Compared with wider spacing, closer tree intervals increased the likelihood that neighboring crowns overlapped or formed near-continuous shade coverage along canal-side walkways, thereby reducing radiant heat exposure during peak summer conditions. The results indicate that spacing and canopy density interacted synergistically rather than independently. Higher-LAI trees produced stronger cooling effects when planted at closer intervals, whereas under wider spacing, even relatively dense canopies often left portions of pedestrian areas exposed to direct solar radiation, limiting reductions in MRT and associated improvements in thermal comfort. The results therefore suggest that the cooling benefit of waterside trees is primarily controlled by the combined influence of canopy density and planting arrangement through their effect on effective shade continuity, rather than by LAI or spacing considered separately. This interaction is consistent with broader evidence suggesting that vegetation cooling may exhibit threshold-like behaviour. For example, Ziter et al. [24] reported that daytime air-temperature cooling became substantially more pronounced when urban canopy cover exceeded approximately 40%, implying that vegetation cooling can increase nonlinearly once canopy coverage reaches sufficient spatial continuity. Although the spatial scale examined by Ziter et al. [24] differs considerably from the canal-edge scenarios investigated here, the broader principle appears applicable: cooling performance may strengthen disproportionately once tree canopies collectively form sufficiently continuous shading structures. This finding reinforces that effective canopy configuration, rather than simply increasing tree numbers or LAI, should be regarded as the primary design objective for improving thermal comfort along canal-edge walkways.

It should also be acknowledged that canopy density was not isolated as an independent variable in this study. The three tested LAI levels were represented by different tree species from the ENVI-met vegetation database rather than by modifying LAI alone while holding tree morphology constant. Consequently, the observed differences should not be attributed solely to crown density, as cooling performance may also have been influenced by species-specific physical characteristics, including tree height, crown geometry, crown size, vertical leaf distribution, and associated aerodynamic effects. Previous studies have similarly shown that tree morphology can strongly influence the balance between shading, evapotranspirative cooling, and pedestrian-level ventilation, all of which jointly determine outdoor thermal comfort [23,120,122,123].

4.5. Implications for Climate-Responsive Canal-Edge Design

4.5.1. Assessing Site Context Before Tree-Planting Interventions

The findings suggest that the synergistic cooling contribution of blue-green elements should not be evaluated independently, but rather understood as part of a broader site-specific microclimatic system shaped by building morphology, shading patterns, and ventilation corridors. It is necessary first to conduct a detailed assessment of the surrounding thermal environment of the waterfront area to form the baseline environmental condition, which serves as a macro-scale background that largely determines the thermal comfort performance of the waterfront space [121]. In terms of surrounding buildings, different orientations create varying shading patterns throughout the day, while also interacting with the local prevailing wind to either enhance or reduce ventilation along the canal-edge pedestrian pathways [25,101,120]. According to Ampatzidis and Kershaw [104], with a narrower range of wind directions, an elongated water body like a canal is more effective due to the greater fetch. To economically maximise shaded areas, a detailed thermal environment analysis should be carried out before tree planting, and trees should be placed in areas outside the zones already covered by building shade throughout the day.

4.5.2. Tree Species Selection for Maximizing Cooling Performance

For tree planting along canal edges, species that can provide extensive shade coverage (i.e., with a broad canopy spread and greater height) while also having relatively dense foliage are considered ideal choices. In addition, because of the proximity to water, tolerance to wet soil conditions should also be taken into account as an important selection criterion. The UK Canal & River Trust identifies five suitable tree types commonly found along canal walks: willows (*Salix* spp.), English oak (*Quercus robur*), common ash (*Fraxinus excelsior*), sycamore (*Acer pseudoplatanus*), and horse chestnut (*Aesculus hippocastanum*) [124]. Furthermore, considering climate change, greater emphasis should be placed on selecting tree species that are more tolerant of relatively higher temperatures and changing climatic conditions.

4.5.3. Activating Canal-Edge Spaces as Attractive Cooling Refuges

Urban canal-edge spaces have significant potential to provide recreational spaces or even heat refuges during heatwave events, while the potential health and well-being benefits of blue-space exposure further support their design as accessible and inviting public spaces [125]. According to the Canal & River Trust, more than 10 million people access green space and nature through the canal network each year [126]. Further consideration is needed regarding how urban regeneration and landscape design can enhance the synergistic cooling effects of blue and green infrastructure while simultaneously attracting greater public use of canal-edge spaces. Due to the linear spatial characteristics of canal-side walkways, these spaces tend to encourage pedestrian movement and passage rather than lingering. Through landscape design interventions, the introduction of features such as seating, pocket plazas, and over-water deck platforms can help transform these areas from primarily movement-oriented spaces into places for staying and leisure, thereby enhancing the vitality and attractiveness of canal-edge environments. As heatwaves become more frequent under climate change, canal-edge spaces may increasingly function as informal climate refuges within dense urban areas, highlighting their importance within broader urban heat adaptation strategies.

4.6. Limitations and Future Work

As a preliminary study exploring canal-edge spaces in the UK, this research has several limitations that should be addressed in future work. First, the design of the canal-edge space in this study was relatively conceptual, considering only the linear walkway along the canal. Other landscape elements where people are more likely to stay for longer periods, such as viewing platforms, stepped seating, and similar waterfront amenities, were not included, even though these spaces may have a greater influence on people's thermal comfort due to prolonged exposure. In addition, this study mainly focused on tree planting along hard-engineered canal embankments. However, in recent years, waterfront landscape design in the UK has increasingly shifted toward more naturalistic embankment treatments, with designers introducing riverside meadow planting and shrub vegetation. Therefore, future research should move beyond the current conceptualised approach and incorporate more realistic canal-edge spatial designs and modelling setups that better reflect contemporary landscape design practices.

5. Conclusions

This study investigated how urban green–blue infrastructure influences the thermal environment of canal-edge pedestrian walkways under extreme summer conditions using a validated ENVI-met model and a parametric analysis of 32 scenarios in Manchester, UK.

The results demonstrate that although both water bodies and riparian trees contribute to improving pedestrian thermal comfort, their cooling performance differs substantially in magnitude and mechanism. Canal water alone provided measurable but relatively limited daytime cooling, with its effectiveness strongly influenced by canal width, orientation and local ventilation conditions. By contrast, riparian trees produced much greater improvements in thermal comfort, primarily through reducing mean radiant temperature via canopy shading. The findings further show that the cooling performance of canal-edge environments depends not only on the presence of blue and green infrastructure, but also on their interaction. Rather than acting as the dominant cooling source, canal water appears to enhance the cooling efficiency of adjacent vegetation by creating favourable microclimatic conditions, while the greatest thermal benefits were achieved where continuous tree shade substantially reduced pedestrian radiant heat exposure.

The study also demonstrates that canopy configuration is more important than individual planting parameters. Higher canopy density and closer planting intervals generally improved thermal comfort, but the relationship was not strictly linear. Instead, cooling increased disproportionately once tree canopies became sufficiently continuous to minimise gaps in pedestrian shading, suggesting the existence of threshold-like behaviour in vegetation cooling performance. These findings indicate that effective canal-edge cooling should be understood as the result of interactions among radiation, airflow, water bodies and vegetation, rather than optimisation of any single design element.

From a practical perspective, the study provides quantitative evidence to support climate-responsive design of canal-edge public spaces in temperate cities. While widening waterways may enhance cooling under favourable morphological conditions, improving shade continuity through appropriate tree configuration is likely to provide a more robust and reliable strategy for reducing pedestrian heat stress. With over 2000 miles of walkable canals in England and Wales, these under-researched areas could potentially provide greater cooling effects both within England and Wales but also more widely across the globe. As heatwaves become increasingly frequent under climate change, integrating water and vegetation through context-sensitive design may help transform urban canal corridors into more thermally comfortable and resilient public spaces.

Author Contributions: Conceptualization, Y.W., Z.L. and P.B.; Methodology, Y.W., Z.L. and P.B.; Software, Y.W.; Validation, Y.W.; Formal Analysis, Y.W., Z.L. and P.B.; Investigation, Y.W.; Data Curation, Y.W.; Writing—Original Draft Preparation, Y.W., Z.L. and P.B.; Writing—Review and Editing, Y.W., Z.L. and P.B.; Visualisation, Y.W. and Z.L. All authors have read and agreed to the published version of the manuscript.

Funding: This research received no external funding.

Institutional Review Board Statement: Not applicable.

Informed Consent Statement: Not applicable.

Data Availability Statement: The datasets generated and/or analysed during the current study are available from the corresponding author upon reasonable request.

Acknowledgments: We would like to sincerely thank Hui Li for her professional advice during the research proposal stage of this study. We would also like to thank Aimee Felstead for her teaching and guidance on academic writing skills during the dissertation module.

Conflicts of Interest: The authors declare no conflicts of interest.

Abbreviations

The following abbreviations are used in this manuscript:

BGI	Blue–green infrastructure
UHI	Urban heat island
TA	Air temperature
RH	Relative humidity
WS	Wind speed
MRT	Mean radiant temperature
PET	Physiological Equivalent Temperature
LAI	Leaf area index

Appendix A

Meteorological forcing data for ENVI-met simulation.

Table A1. Simulation area and date: Manchester, 19 July 2022.

Simulation Hour	Time	Air Temperature (°C)	Wind (m/s)	Wind Direction	Relative Humidity (%)
0	08:50	31.1	0.89	↓	29
0.5	09:20	32.2	1.34	↑	29
1	09:50	31.1	1.34	↖	29
1.5	10:20	32.8	3.13	↖	26
2	10:50	33.9	2.68	↑	24
2.5	11:20	33.9	2.68	↑	24
3	11:50	35	2.68	↖	25
3.5	12:20	35	3.58	↑	25
4	12:50	36.1	3.58	↑	23
4.5	13:20	36.1	3.58	↑	23
5	13:50	37.2	3.58	↑	21
5.5	14:20	37.8	4.47	↗	20
6	14:50	37.2	7.15	↗	24
6.5	15:20	35	8.05	→	30
7	15:50	33.9	7.6	→	28
7.5	16:20	32.8	6.71	→	30
8	16:50	32.2	5.36	↘	31

Source: Weather data for Manchester on 19 July 2022 were obtained from Time and Date [62]. Temperatures were converted from degrees Fahrenheit to degrees Celsius.

Appendix B

Table A2. The information on the six studied canal cases in Manchester city centre.

Typology	Reference Reach	Typical Canal Width	Dominant Orientation
Narrow, highly built-up canal canyon	Bridgewater Canal – Deansgate Locks	8–12 m	WN–ES
Narrow, highly built-up canal canyon	Rochdale Canal – Canal Street	8–12 m	WN–ES
Narrow, highly built-up canal canyon	Ashton Canal	10–12 m	WN–ES
Medium-width basin nodes	Castlefield Basin	20–30 m interconnected basins	Mixed (radial)
Medium-width basin nodes	Piccadilly Basin	25–30 m	E–W
Wide urban waterbody	New Islington	7–20 m	Minor E–W axis

Source: Compiled from field observations and data from Waterpride Estates Ltd. [50] and Deloitte Real Estate [73], with canal-design context informed by Verheij [74].

Appendix C

Table A3. Scenario settings.

	Canal Orientation	Canal Width	Canal with Water?	Planting Interval	Leaf Area Index (LAI)	Tree Species
Scenario with blue-green elements 1	N–S	Narrow (8 m)	✓	10 m	Low LAI (1.5)	*Sorbus arnoldiana*
Scenario with blue-green elements 2	N–S	Narrow (8 m)	✓	10 m	Medium LAI (3)	*Betula pendula*
Scenario with blue-green elements 3	N–S	Narrow (8 m)	✓	10 m	High LAI (5)	*Tilia × europaea*
Scenario with blue-green elements 4	N–S	Narrow (8 m)	✓	5 m	Low LAI (1.5)	*Sorbus arnoldiana*
Scenario with blue-green elements 5	N–S	Narrow (8 m)	✓	5 m	Medium LAI (3)	*Betula pendula*
Scenario with blue-green elements 6	N–S	Narrow (8 m)	✓	5 m	High LAI (5)	*Tilia × europaea*
Scenario with blue-green elements 7	E–W	Narrow (8 m)	✓	10 m	Low LAI (1.5)	*Sorbus arnoldiana*
Scenario with blue-green elements 8	E–W	Narrow (8 m)	✓	10 m	Medium LAI (3)	*Betula pendula*
Scenario with blue-green elements 9	E–W	Narrow (8 m)	✓	10 m	High LAI (5)	*Tilia × europaea*
Scenario with blue-green elements 10	E–W	Narrow (8 m)	✓	5 m	Low LAI (1.5)	*Sorbus arnoldiana*
Scenario with blue-green elements 11	E–W	Narrow (8 m)	✓	5 m	Medium LAI (3)	*Betula pendula*
Scenario with blue-green elements 12	E–W	Narrow (8 m)	✓	5 m	High LAI (5)	*Tilia × europaea*
Scenario with blue-green elements 13	N–S	Wide (20 m)	✓	10 m	Low LAI (1.5)	*Sorbus arnoldiana*
Scenario with blue-green elements 14	N–S	Wide (20 m)	✓	10 m	Medium LAI (3)	*Betula pendula*
Scenario with blue-green elements 15	N–S	Wide (20 m)	✓	10 m	High LAI (5)	*Tilia × europaea*
Scenario with blue-green elements 16	N–S	Wide (20 m)	✓	5 m	Low LAI (1.5)	*Sorbus arnoldiana*
Scenario with blue-green elements 17	N–S	Wide (20 m)	✓	5 m	Medium LAI (3)	*Betula pendula*
Scenario with blue-green elements 18	N–S	Wide (20 m)	✓	5 m	High LAI (5)	*Tilia × europaea*
Scenario with blue-green elements 19	E–W	Wide (20 m)	✓	10 m	Low LAI (1.5)	*Sorbus arnoldiana*
Scenario with blue-green elements 20	E–W	Wide (20 m)	✓	10 m	Medium LAI (3)	*Betula pendula*
Scenario with blue-green elements 21	E–W	Wide (20 m)	✓	10 m	High LAI (5)	*Tilia × europaea*
Scenario with blue-green elements 22	E–W	Wide (20 m)	✓	5 m	Low LAI (1.5)	*Sorbus arnoldiana*
Scenario with blue-green elements 23	E–W	Wide (20 m)	✓	5 m	Medium LAI (3)	*Betula pendula*
Scenario with blue-green elements 24	E–W	Wide (20 m)	✓	5 m	High LAI (5)	*Tilia × europaea*
Reference Scenario 1	N–S	Narrow (8 m)	No water	/	/	/
Reference Scenario 2	E–W	Narrow (8 m)	No water	/	/	/
Reference Scenario 3	N–S	Wide (20 m)	No water	/	/	/

Table A3. *Cont.*

	Canal Orientation	Canal Width	Canal with Water?	Planting Interval	Leaf Area Index (LAI)	Tree Species
Reference Scenario 4	E–W	Wide (20 m)	No water	/	/	/
Scenario with water only 1	N–S	Narrow (8 m)	✓	/	/	/
Scenario with water only 2	E–W	Narrow (8 m)	✓	/	/	/
Scenario with water only 3	N–S	Wide (20 m)	✓	/	/	/
Scenario with water only 4	E–W	Wide (20 m)	✓	/	/	/

Appendix D

Table A4. The statistical metrics for tree-shaded and unshaded sites in ENVI-met validation.

	Site	R^2	RMSE	MAE	MBE
TA (°C)	**Tree-shaded** **Unshaded**	0.99 0.85	0.50 1.11	0.40 0.59	+0.06 −0.55
RH (%)	**Tree-shaded** **Unshaded**	0.86 0.91	2.26 1.84	1.82 1.33	+1.51 −0.03

References

1. Met Office. *Unprecedented Extreme Heatwave, July 2022: Event Summary*; Met Office: Exeter, UK, 2022. Available online: https://www.metoffice.gov.uk/binaries/content/assets/metofficegovuk/pdf/weather/learn-about/uk-past-events/interesting/2022/\2022_03_july_heatwave_v1.pdf (accessed on 22 September 2025).
2. van Daalen, K.R.; Tonne, C.; Semenza, J.C.; Rocklov, J.; Markandya, A.; Dasandi, N.; Jankin, S.; Achebak, H.; Ballester, J.; Bechara, H.; et al. The 2024 Europe report of the Lancet Countdown on health and climate change: Unprecedented warming demands unprecedented action. *Lancet Public Health* **2024**, *9*, e495–e522. [CrossRef] [PubMed]
3. Beddow, H. How the Urban Heat Island Effect Makes Cities Vulnerable to Climate Change. UK Green Building Council. 15 August 2022. Available online: https://ukgbc.org/news/how-the-urban-heat-island-effect-makes-cities-vulnerable-to-climate-change/ (accessed on 31 July 2026).
4. IPCC. Chapter 8: Urban systems and other settlements. In *Climate Change 2022: Mitigation of Climate Change. Contribution of Working Group III to the Sixth Assessment Report of the Intergovernmental Panel on Climate Change*; Cambridge University Press: Cambridge, UK; New York, NY, USA, 2022; pp. 861–952. [CrossRef]
5. European Commission. *Green Infrastructure (GI): Enhancing Europe's Natural Capital*; COM(2013) 249 final; European Commission: Brussels, Belgium, 2013. Available online: https://eur-lex.europa.eu/legal-content/EN/TXT/?uri=CELEX%3A52013DC0249 (accessed on 3 May 2026).
6. Ghofrani, Z.; Sposito, V.; Faggian, R. A comprehensive review of blue-green infrastructure concepts. *Int. J. Environ. Sustain.* **2017**, *6*, 15–36. [CrossRef]
7. CIRIA. *Blue-Green Infrastructure: Perspectives on Planning, Evaluation and Collaboration (C780a)*; CIRIA: London, UK, 2019. Available online: https://www.ciria.org/Books/Free_publications/C780F.aspx (accessed on 3 May 2026).
8. Veerkamp, C.J.; Schipper, A.M.; Hedlund, K.; Lazarova, T.; Nordin, A.; Hanson, H.I. A review of studies assessing ecosystem services provided by urban green and blue infrastructure. *Ecosyst. Serv.* **2021**, *52*, 101367. [CrossRef]
9. Directorate-General for Environment. Using Blue-Green Infrastructure in Cities Increases Regional Habitat Connectivity and Benefits Biodiversity. 2022. Available online: https://environment.ec.europa.eu/news/using-blue-green-infrastructure-cities-increases-regional-habitat-connectivity-and-benefits-2022-11-16_en (accessed on 30 July 2026).
10. Geary, R.S.; Thompson, D.A.; Garrett, J.K.; Mizen, A.; Rowney, F.M.; Song, J.; White, M.P.; Lovell, R.; Watkins, A.; Lyons, R.A.; et al. Green–blue space exposure changes and impact on individual-level well-being and mental health: A population-wide dynamic longitudinal panel study with linked survey data. *Public Health Res.* **2023**, *11*, 1–176. [CrossRef] [PubMed]
11. Canal & River Trust. *Towpaths for Everyone: Our Policy for Designing and Managing Towpaths as Shared Spaces for Everyone to Enjoy*; Canal & River Trust: Ellesmere Port, UK, 2024. Available online: https://canalrivertrust.org.uk/media/document/Mn2jc9w8d4LJqw-8tlUGKA/sK34Z1Bz2I9UTGudATIMmeneKoVwARlrUflG5otmJvE/aHR0cHM6Ly9jcnRwcm9kY21zdWtzMDEuYmxvYi5jb3JlLndpbmRvd3MubmV0L2RvY3VtZW50Lw/018972f7-1ac0-7ffb-b333-e500e22f7f25.pdf (accessed on 30 July 2026).
12. Cycling UK. *Towpaths, Canals and Rivers*; Campaigns Briefing 5J; Cycling UK: Guildford, UK, 2017. Available online: https://www.cyclinguk.org/sites/default/files/document/migrated/info/towpaths5jbrf.pdf (accessed on 30 July 2026).

13. Woolf, Y.; Short, M. From industry to greenery: Exploring how users experience the Regent's Canal. *Front. Sustain. Cities* **2025**, *7*, 1498698. [CrossRef]
14. London Legacy Development Corporation. LLDC Green Infrastructure Guide Published to Share Best Practice and Learning. Queen Elizabeth Olympic Park. 21 January 2022. Available online: https://www.queenelizabetholympicpark.co.uk/our-stories/lldc-green-infrastructure-guide-published-share-best-practice-and-learning (accessed on 4 May 2026).
15. London Legacy Development Corporation. Queen Elizabeth Olympic Park: Park Design Guide 2024. 2024. Available online: https://www.queenelizabetholympicpark.co.uk/about-us/how-we-work/park-design-guide (accessed on 4 May 2026).
16. Cao, B.; Chen, Q.; Du, M.; Cheng, Q.; Li, Y.; Liu, R. Simulation analysis of the cooling effect of urban water bodies on the local thermal environment. *Water* **2022**, *14*, 3091. [CrossRef]
17. Cheng, Y.; Shen, L.; Teng, M.; Liu, H.; Cheng, W.; Zhang, B.; Wu, C. How to use lake breeze circulations to improve urban natural ventilation: A case study in a typical inland multi-lake megacity. *Landsc. Urban Plan.* **2023**, *230*, 104628. [CrossRef]
18. Fang, Y.; Gu, K.; Qian, Z.; Sun, Z.; Wang, Y.; Wang, A. Performance evaluation on multi-scenario urban ventilation corridors based on least cost path. *J. Urban Manag.* **2021**, *10*, 3–15. [CrossRef]
19. Li, X.; Lin, K.; Shu, Y.; Lin, X. Comparison of the influences of different ventilation corridor forms on the thermal environment in Wuhan City in summer. *Sci. Rep.* **2023**, *13*, 13416. [CrossRef] [PubMed]
20. Wong, N.H.; Tan, C.L.; Kolokotsa, D.D.; Takebayashi, H. Greenery as a mitigation and adaptation strategy to urban heat. *Nat. Rev. Earth Environ.* **2021**, *2*, 166–181. [CrossRef]
21. Knight, T.; Price, S.; Bowler, D.; Hookway, A.; King, S.; Konno, K.; Richter, R.L. How effective is 'greening' of urban areas in reducing human exposure to ground-level ozone concentrations, UV exposure and the 'urban heat island effect'? An updated systematic review. *Environ. Evid.* **2021**, *10*, 12. [CrossRef]
22. Chen, J.; Huang, Y.; Porter, D.; Neri, E. Urban vegetation design recommendation for improving outdoor thermal comfort in tropical and temperate climate zones. In Proceedings of the Building Simulation 2023: 18th Conference of IBPSA, Shanghai, China, 4–6 September 2023; pp. 517–524. [CrossRef]
23. Meili, N.; Manoli, G.; Burlando, P.; Carmeliet, J.; Chow, W.T.; Coutts, A.M.; Roth, M.; Velasco, E.; Vivoni, E.R.; Fatichi, S. Tree effects on urban microclimate: Diurnal, seasonal, and climatic temperature differences explained by separating radiation, evapotranspiration, and roughness effects. *Urban For. Urban Green.* **2021**, *58*, 126970. [CrossRef]
24. Ziter, C.D.; Pedersen, E.J.; Kucharik, C.J.; Turner, M.G. Scale-dependent interactions between tree canopy cover and impervious surfaces reduce daytime urban heat during summer. *Proc. Natl. Acad. Sci. USA* **2019**, *116*, 7575–7580. [CrossRef] [PubMed]
25. Lee, H.; Mayer, H.; Kuttler, W. Impact of the spacing between tree crowns on the mitigation of daytime heat stress for pedestrians inside E–W urban street canyons under Central European conditions. *Urban For. Urban Green.* **2020**, *48*, 126558. [CrossRef]
26. Liu, J.; Zheng, B.; Yang, F. A simulation study of the impact of urban street greening on the thermal comfort in street canyons on hot and cold days. *Forests* **2023**, *14*, 2256. [CrossRef]
27. Shi, D.; Song, J.; Huang, J.; Zhuang, C.; Guo, R.; Gao, Y. Synergistic cooling effects (SCEs) of urban green-blue spaces on local thermal environment: A case study in Chongqing, China. *Sustain. Cities Soc.* **2020**, *55*, 102065. [CrossRef]
28. Wang, M.; Song, H.; Zhu, W.; Wang, Y. The cooling effects of landscape configurations of green–blue spaces in urban waterfront community. *Atmosphere* **2023**, *14*, 833. [CrossRef]
29. Robitu, M.; Musy, M.; Inard, C.; Groleau, D. Modeling the influence of vegetation and water pond on urban microclimate. *Sol. Energy* **2006**, *80*, 435–447. [CrossRef]
30. Qiu, X.; Kil, S.-H.; Jo, H.-K.; Park, C.; Song, W.; Choi, Y.E. Cooling effect of urban blue and green spaces: A case study of Changsha, China. *Int. J. Environ. Res. Public Health* **2023**, *20*, 2613. [CrossRef] [PubMed]
31. Fricke, L.; Legg, R.; Kabisch, N. Impact of blue spaces on the urban microclimate in different climate zones, daytimes and seasons—A systematic review. *Urban For. Urban Green.* **2024**, *101*, 128528. [CrossRef]
32. Sanusi, R.; Johnstone, D.; May, P.; Livesley, S.J. Street orientation and side of the street greatly influence the microclimatic benefits street trees can provide in summer. *J. Environ. Qual.* **2016**, *45*, 167–174. [CrossRef] [PubMed]
33. Gangwisch, M.; Fröhlich, D.; Christen, A.; Matzarakis, A. Geometrical assessment of sunlit and shaded area of urban trees based on aligned orthographic views. *Atmosphere* **2021**, *12*, 968. [CrossRef]
34. Ng, E.; Yuan, C.; Chen, L.; Ren, C.; Fung, J.C. Improving the wind environment in high-density cities by understanding urban morphology and surface roughness: A study in Hong Kong. *Landsc. Urban Plan.* **2011**, *101*, 59–74. [CrossRef] [PubMed]
35. Jiang, Y.; Huang, J.; Shi, T.; Li, X. Cooling island effect of blue-green corridors: Quantitative comparison of morphological impacts. *Int. J. Environ. Res. Public Health* **2021**, *18*, 11917. [CrossRef] [PubMed]
36. Jacobs, C.; Klok, L.; Bruse, M.; Cortesão, J.; Lenzholzer, S.; Kluck, J. Are urban water bodies really cooling? *Urban Clim.* **2020**, *32*, 100607. [CrossRef]
37. Völker, S.; Baumeister, H.; Claßen, T.; Hornberg, C.; Kistemann, T. Evidence for the temperature-mitigating capacity of urban blue space—A health geographic perspective. *Erdkunde* **2013**, *67*, 355–371. [CrossRef]

38. Jiang, Y.; Song, D.; Shi, T.; Han, X. Adaptive analysis of green space network planning for the cooling effect of residential blocks in summer: A case study in Shanghai. *Sustainability* **2018**, *10*, 3189. [CrossRef]
39. McDonald, H.; Chambers, J.; Taylor, S.; Johnston, B.; Coogan, N.; Adebowale, O.; Tippett, J.; Huck, J.; Walter, M. *The Urban Cooling Effect of Canals in Cities Shown to Exceed 1 Degree Centigrade in Summer: Canals, Cooling and Replicable Models—Summary Report to the Canal & River Trust*; School of Environment, Education and Development, The University of Manchester: Manchester, UK, 2019. Available online: https://documents.manchester.ac.uk/display.aspx?DocID=57300 (accessed on 31 July 2026).
40. Afentou, N.; Moore, P.; Hull, K.; Shepherd, J.; Elliott, S.; Frew, E. Inland waterways and population health and wellbeing: A cross-sectional study of waterway users in the UK. *Int. J. Environ. Res. Public Health* **2022**, *19*, 13809. [CrossRef] [PubMed]
41. Waterfront Alliance. About WEDG. Waterfront Alliance. Available online: https://wedg.waterfrontalliance.org/about/ (accessed on 21 September 2025).
42. Wang, X. *Guidelines on Integrating Nature-Based Passive Cooling Options into Urban Planning and Design*; ESMAP Paper, Report No. 180030; World Bank Group: Washington, DC, USA, 2023. Available online: https://documents.worldbank.org/en/publication/documents-reports/documentdetail/099341202212324606 (accessed on 21 September 2025).
43. Jandaghian, Z.; Colombo, A. The role of water bodies in climate regulation: Insights from recent studies on urban heat island mitigation. *Buildings* **2024**, *14*, 2945. [CrossRef]
44. Kottek, M.; Grieser, J.; Beck, C.; Rudolf, B.; Rubel, F. World map of the Köppen-Geiger climate classification updated. *Meteorol. Z.* **2006**, *15*, 259–263. [CrossRef] [PubMed]
45. Beck, H.E.; Zimmermann, N.E.; McVicar, T.R.; Vergopolan, N.; Berg, A.; Wood, E.F. Present and future Köppen-Geiger climate classification maps at 1-km resolution. *Sci. Data* **2018**, *5*, 180214. [CrossRef] [PubMed]
46. Met Office. A Milestone in UK Climate History. 22 July 2022. Available online: https://www.metoffice.gov.uk/about-us/news-and-media/media-centre/weather-and-climate-news/2022/july-heat-review (accessed on 30 July 2026).
47. Manchester City Council. *Heatwaves and Health Report*; Report to Health Scrutiny Committee; Manchester City Council: Manchester, UK, 7 December 2022. Available online: https://democracy.manchester.gov.uk/documents/s37243/Heatwaves%20and%20Health%20Report.pdf (accessed on 30 July 2026).
48. Met Office Press Office. UK Prepares for Historic Hot Spell. 15 July 2022. Available online: https://www.metoffice.gov.uk/about-us/news-and-media/media-centre/weather-and-climate-news/2022/red-extreme-heat-warning (accessed on 23 September 2025).
49. Canal & River Trust. *North West 2025 (Regional Overview—Manchester Section)*; Canal & River Trust: Ellesmere Port, UK, 2025. Available online: https://canalrivertrust.org.uk/media/document/4xoPuqBX2AgAeCNgAwDrWg/cJmsWEiuBepdYzmHynle7fE0cQtoRGHyAxGSdMC68mg/aHR0cHM6Ly9jcnRwcm9kY21zdWtzMDEuYmxvYi5jb3JlLndpbmRvd3MubmV0L2RvY3VtZW50Lw/0196c9ef-ae7d-7ac0-8bed-b81ea8d67933.pdf (accessed on 22 September 2025).
50. Waterpride Estates Ltd. New Islington Marina. Available online: https://www.waterwayleisure.com/new-islington-marina (accessed on 22 September 2025).
51. Liu, Z.; Cheng, W.; Jim, C.Y.; Morakinyo, T.E.; Shi, Y.; Ng, E. Heat mitigation benefits of urban green and blue infrastructures: A systematic review of modeling techniques, validation and scenario simulation in ENVI-met V4. *Build. Environ.* **2021**, *200*, 107939. [CrossRef]
52. Bruse, M.; Fleer, H. Simulating surface–plant–air interactions inside urban environments with a three dimensional numerical model. *Environ. Model. Softw.* **1998**, *13*, 373–384. [CrossRef]
53. Ouyang, W.; Morakinyo, T.E.; Ren, C.; Ng, E. The cooling efficiency of variable greenery coverage ratios in different urban densities: A study in a subtropical climate. *Build. Environ.* **2020**, *174*, 106772. [CrossRef]
54. Liu, Z.; Zheng, S.; Zhao, L. Evaluation of the ENVI-Met vegetation model of four common tree species in a subtropical hot-humid area. *Atmosphere* **2018**, *9*, 198. [CrossRef]
55. Time and Date AS. Weather in August 2025 in Manchester, England, United Kingdom. Available online: https://www.timeanddate.com/weather/uk/manchester/historic?month=8&year=2025 (accessed on 31 July 2026).
56. Liu, Z.; Cheng, K.Y.; He, Y.; Jim, C.Y.; Brown, R.D.; Shi, Y.; Lau, K.; Ng, E. Microclimatic measurements in tropical cities: Systematic review and proposed guidelines. *Build. Environ.* **2022**, *222*, 109411. [CrossRef]
57. Hodson, T.O. Root-mean-square error (RMSE) or mean absolute error (MAE): When to use them or not. *Geosci. Model Dev.* **2022**, *15*, 5481–5487. [CrossRef]
58. *EPA-454/R-99-005*; Meteorological Monitoring Guidance for Regulatory Modeling Applications. U.S. Environmental Protection Agency, Office of Air Quality Planning and Standards: Research Triangle Park, NC, USA, 2000. Available online: https://www.epa.gov/scram/air-modeling-meteorological-guidance (accessed on 31 July 2026).
59. Rennie, J.J.; Palecki, M.A.; Heuser, S.P.; Diamond, H.J. Developing and validating heat exposure products using the US climate reference network. *J. Appl. Meteorol. Clim.* **2021**, *60*, 543–558. [CrossRef]
60. Willmott, C.J. Some comments on the evaluation of model performance. *Bull. Am. Meteorol. Soc.* **1982**, *63*, 1309–1313. [CrossRef]

61. Stunder, M.; Sethuraman, S. A statistical evaluation and comparison of coastal point source dispersion models. *Atmos. Environ.* **1986**, *20*, 301–315. [CrossRef]
62. Time and Date. Weather in July 2022 in Manchester, England, United Kingdom. Available online: https://www.timeanddate.com/weather/uk/manchester/historic?month=7&year=2022 (accessed on 4 September 2025).
63. Fiorillo, E.; Brilli, L.; Carotenuto, F.; Cremonini, L.; Gioli, B.; Giordano, T.; Nardino, M. Diurnal outdoor thermal comfort mapping through ENVI-met simulations, remotely sensed and in situ measurements. *Atmosphere* **2023**, *14*, 641. [CrossRef]
64. Manchester City Council. *Poland Street Zone: Neighbourhood Development Framework Addendum—Public Realm Strategy*; Manchester City Council: Manchester, UK, 2022. Available online: https://www.manchester.gov.uk/download/downloads/id/28231/draft_public_realm_strategy.pdf (accessed on 3 September 2025).
65. Science and Industry Museum. The World's First Industrial City. 2025. Available online: https://www.scienceandindustrymuseum.org.uk/objects-and-stories/worlds-first-industrial-city (accessed on 30 July 2026).
66. Canal & River Trust. *Guidance for Towpath Design, Version 2*; Canal & River Trust: Ellesmere Port, UK, 2013. Available online: https://canalrivertrust.org.uk/media/document/nQXi20gNJAhPpE3Y9t2dGQ/GDD3atG_rPl0-fzNBn6E_6lRsbO4fdp3wePqawCJmLY/aHR0cHM6Ly9jcnRwcm9kY21zdWtzMDEuYmxvYi5jb3JlLndpbmRvd3MubmV0L2RvY3\VtZW50Lw/0189d4bd-245a-754e-8d07-f38c6356994c.pdf (accessed on 22 September 2025).
67. Active Travel England. Shared Use. 2019. Available online: https://www.activetravelengland.gov.uk/planning-active-places/shared-use (accessed on 3 September 2025).
68. FCBStudios.com. FeildenCleggBradley Studios. 2025. Available online: https://fcbstudios.com/projects/murrays-mills-manchester/ (accessed on 3 September 2025).
69. Historic England. Merchants Warehouse. Historic England Research Records, Hob UID: 1056620. Available online: https://www.heritagegateway.org.uk/Gateway/Results_Single.aspx?resourceID=19191&uid=1056620 (accessed on 3 September 2025).
70. Met Office. Where Are the Windiest Parts of the UK? Available online: https://weather.metoffice.gov.uk/learn-about/weather/types-of-weather/wind/windiest-place-in-uk (accessed on 17 September 2025).
71. Xu, W.; Zhao, L.; Zhang, Y.; Gu, Z. Investigation on Air Ventilation within Idealised Urban Wind Corridors and the Influence of Structural Factors with Numerical Simulations. *Sustainability* **2023**, *15*, 13817. [CrossRef]
72. Ai, Z.; Mak, C.M. CFD simulation of flow in a long street canyon under a perpendicular wind direction: Evaluation of three computational settings. *Build. Environ.* **2017**, *114*, 293–306. [CrossRef]
73. Deloitte Real Estate. *Piccadilly Basin Strategic Regeneration Framework*; Deloitte Real Estate: London, UK, 2016. Available online: https://www.manchester.gov.uk/__data/assets/file/0025/125359/piccadilly_basin_srf_28_october_2016_final.pdf (accessed on 22 September 2025).
74. Verheij, H. *Hydraulic Aspects of the Montgomery Canal Restoration*; Report Q3967; WL | Delft Hydraulics: Delft, The Netherlands, 2006; prepared for British Waterways. Available online: https://canalrivertrust.org.uk/media/document/CD7mFM4dyv-HYXiDQJQo_g/fzRdDDppUB1BB25LZTr71qZGEUnauT0Q0gNcC7TDk_U/aHR0cHM6Ly9jcnRwcm9kY21zdWtzMDEuYmxvYi5jb3JlLndpbmRvd3MubmV0L2RvY3VtZW50Lw/0189d4be-3156-7156-a5a0-e7feee08e5fc.pdf (accessed on 22 September 2025).
75. Canal & River Trust. Boating the Ashton Canal. 2025. Available online: https://canalrivertrust.org.uk/canals-and-rivers/ashton-canal/boating-the-ashton-canal (accessed on 3 September 2025).
76. Wilts & Berks Canal Trust. *Engineering Specification and Design Guidance*; Version 1.0; Wilts & Berks Canal Trust: Chippenham, UK, 2018. Available online: https://www.canalpartnership.org.uk/files/studies/WBCTEngSpecV1.pdf (accessed on 3 September 2025).
77. Tikkanen, A. Manchester Ship Canal. Encyclopaedia Britannica. Available online: https://www.britannica.com/topic/Manchester-Ship-Canal (accessed on 30 July 2026).
78. Environment Agency. *Managing Flood Risk: Irwell Catchment Flood Management Plan*; Environment Agency: Bristol, UK, 2009. Available online: https://assets.publishing.service.gov.uk/media/5a7c812e40f0b626628ac87d/Irwell_Catchment_Flood_Manage\ment_Plan.pdf (accessed on 30 July 2026).
79. Department for Transport. *Manual for Streets*; Department for Transport: London, UK, 2007; p. 32. Available online: https://assets.publishing.service.gov.uk/media/5a7e0035ed915d74e6223743/pdfmanforstreets.pdf (accessed on 30 July 2026).
80. Leeds City Council. Planting Checklist. Available online: https://www.leeds.gov.uk/planning/conservation-protection-and-heritage/landscape-planning-and-development/planting-checklist (accessed on 5 May 2026).
81. Armson, D.; Rahman, M.A.; Ennos, A.R. A comparison of the shading effectiveness of five different street tree species in Manchester, UK. *Arboric. Urban For.* **2013**, *39*, 157–164. [CrossRef]
82. Moser-Reischl, A.; Franceschi, E.; Rahman, M.A.; Rodrigues-Leite, J.; Pretzsch, H.; Pauleit, S.; Rötzer, T. Spatial and temporal dynamics of the leaf area index (LAI) of selected tree species in urban environments. *Urban For. Urban Green.* **2025**, *107*, 128795. [CrossRef]

83. City of Trees. *All Our Trees: Greater Manchester's Tree & Woodland Strategy*; City of Trees: Manchester, UK, 2024. Available online: https://gmgreencity.com/resource_library/all-our-trees-greater-manchesters-tree-woodland-strategy/ (accessed on 30 July 2026).
84. Fini, A.; Vigevani, I.; Corsini, D.; Wężyk, P.; Bajorek-Zydroń, K.; Failla, O.; Cagnolati, E.; Mielczarek, L.; Comin, S.; Gibin, M.; et al. CO_2-assimilation, sequestration, and storage by urban woody species growing in parks and along streets in two climatic zones. *Sci. Total Environ.* **2023**, *903*, 166198. [CrossRef] [PubMed]
85. *BS 8545:2014*; Trees: From Nursery to Independence in the Landscape—Recommendations. BSI: London, UK, 2014. Available online: https://knowledge.bsigroup.com/products/trees-from-nursery-to-independence-in-the-landscape-recommendations (accessed on 8 July 2026).
86. Trees and Design Action Group. *Trees in Hard Landscapes: A Guide for Delivery*; Trees and Design Action Group: London, UK, 2014. Available online: https://www.tdag.org.uk/trees-in-hard-landscapes.html (accessed on 8 July 2026).
87. Leeds City Council. *LCC Guidance: Urban Tree Planting*; Leeds City Council: Leeds, UK, 2018. Available online: https://www.leeds.gov.uk/sites/default/files/docs/Guidance%20Urban%20Tree%20Planting.pdf (accessed on 8 July 2026).
88. Popplewell, T. *Growing Manchester's Trees: Manchester City Council Tree Planting Capacity Study*; Document Ref. 8386.021; The Environment Partnership: Warrington, UK, 2022; prepared for Manchester City Council. Available online: https://www.manchester.gov.uk/__data/assets/file/0022/125257/growing_manchesters_trees.pdf (accessed on 31 July 2026).
89. ACD Environmental. Tree Pits. 2017. Available online: https://acdenvironmental.co.uk/tree-pits/ (accessed on 30 July 2026).
90. Pépinières Thuilleaux. Sorbus × arnoldiana 'Schouten': Sorbier des oiseaux 'Schouten'. Available online: https://www.thuilleaux.com/arbres-forme-arrondie-1/sorbus-x-arnoldiana-schouten{-}{-}228.html (accessed on 5 May 2026).
91. Keele University. Species Accounts. 2025. Available online: https://www.keele.ac.uk/arboretum/ourtrees/speciesaccounts/ (accessed on 5 May 2026).
92. Plant Photo Bank of China (PPBC). Plant Image No. 27466083 [Photograph]. 23 April 2026. Available online: https://ppbc.iplant.cn/tu/27466083 (accessed on 5 May 2026).
93. Thorsson, S.; Rayner, D.; Lindberg, F.; Monteiro, A.; Katzschner, L.; Lau, K.K.-L.; Campe, S.; Katzschner, A.; Konarska, J.; Onomura, S.; et al. Present and projected future mean radiant temperature for three European cities. *Int. J. Biometeorol.* **2017**, *61*, 1531–1543. [CrossRef] [PubMed]
94. Abdollahzadeh, N.; Biloria, N. Outdoor thermal comfort: Analyzing the impact of urban configurations on the thermal performance of street canyons in the humid subtropical climate of Sydney. *Front. Arch. Res.* **2021**, *10*, 394–409. [CrossRef]
95. Höppe, P. The physiological equivalent temperature—A universal index for the biometeorological assessment of the thermal environment. *Int. J. Biometeorol.* **1999**, *43*, 71–75. [CrossRef] [PubMed]
96. Matzarakis, A.; Mayer, H.; Iziomon, M.G. Applications of a universal thermal index: Physiological equivalent temperature. *Int. J. Biometeorol.* **1999**, *43*, 76–84. [CrossRef] [PubMed]
97. Taleghani, M.; Berardi, U. The effect of pavement characteristics on pedestrians' thermal comfort in Toronto. *Urban Clim.* **2018**, *24*, 449–459. [CrossRef]
98. Crank, P.J.; Sailor, D.J.; Ban-Weiss, G.; Taleghani, M. Evaluating the ENVI-met microscale model for suitability in analysis of targeted urban heat mitigation strategies. *Urban Clim.* **2018**, *26*, 188–197. [CrossRef]
99. Verein Deutscher Ingenieure. *VDI 3787 Blatt 2: Environmental Meteorology—Methods for the Human Biometeorological Evaluation of Climate and Air Quality for Urban and Regional Planning at Regional Level—Part I: Climate*; Verein Deutscher Ingenieure: Düsseldorf, Germany, 2008. Available online: https://www.dinmedia.de/en/technical-rule/vdi-3787-blatt-2/110541685 (accessed on 11 September 2025).
100. Yin, S.; Lang, W.; Xiao, Y. The synergistic effect of street canyons and neighbourhood layout design on pedestrian-level thermal comfort in hot-humid area of China. *Sustain. Cities Soc.* **2019**, *49*, 101571. [CrossRef]
101. Ali-Toudert, F.; Mayer, H. Numerical study on the effects of aspect ratio and orientation of an urban street canyon on outdoor thermal comfort in hot and dry climate. *Build. Environ.* **2006**, *41*, 94–108. [CrossRef]
102. Shashua-Bar, L.; Hoffman, M.E. Geometry and orientation aspects in passive cooling of canyon streets with trees. *Energy Build.* **2003**, *35*, 61–68. [CrossRef]
103. University of Manchester. Research Suggests Canals Can Help the UK to Cope with the Climate Emergency. The University of Manchester, Manchester, UK, 20 October 2021. Available online: https://www.manchester.ac.uk/about/news/canals-can-help-the-uk/ (accessed on 3 September 2025).
104. Ampatzidis, P.; Kershaw, T. A review of the impact of blue space on the urban microclimate. *Sci. Total Environ.* **2020**, *730*, 139068. [CrossRef] [PubMed]
105. Yao, L. Study on the Thermal Effects of Static Urban Water Bodies in Hot-Humid Regions. Ph.D. Thesis, South China University of Technology, Guangzhou, China, 2023.
106. Teshnehdel, S.; Gatto, E.; Li, D.; Brown, R.D. Improving outdoor thermal comfort in a steppe climate: Effect of water and trees in an urban park. *Land* **2022**, *11*, 431. [CrossRef]

107. Met Office. Climate Change in the UK. Available online: https://weather.metoffice.gov.uk/climate-change/climate-change-in-the-uk (accessed on 9 July 2026).
108. Baldwin, J.W.; Benmarhnia, T.; Ebi, K.L.; Jay, O.; Lutsko, N.J.; Vanos, J.K. Humidity's role in heat-related health outcomes: A heated debate. *Environ. Health Perspect.* **2023**, *131*, 055001. [CrossRef] [PubMed]
109. Armson, D.; Stringer, P.; Ennos, A.R. The effect of tree shade and grass on surface and globe temperatures in an urban area. *Urban For. Urban Green.* **2012**, *11*, 245–255. [CrossRef]
110. Park, C.Y.; Lee, D.K.; Krayenhoff, E.S.; Heo, H.K.; Ahn, S.; Asawa, T.; Murakami, A.; Kim, H.G. A multilayer mean radiant temperature model for pedestrians in a street canyon with trees. *Build. Environ.* **2018**, *141*, 298–309. [CrossRef]
111. Schrodi, S.; Briegel, F.; Argus, M.J.; Christen, A.; Brox, T. Climate-sensitive urban planning through optimization of tree placements. In Proceedings of the NeurIPS 2023 Workshop on Tackling Climate Change with Machine Learning, New Orleans, LA, USA, 15–16 December 2023. Available online: https://www.climatechange.ai/papers/neurips2023/30 (accessed on 19 July 2026).
112. Oke, T.R. The micrometeorology of the urban forest. *Philos. Trans. R. Soc. Lond. B Biol. Sci.* **1989**, *324*, 335–349. [CrossRef]
113. Vakilinezhad, R.; Raisi, R.; Ahmadizadeh, O. Evaluating the effect of water body and tree arrangement on courtyard microclimate and outdoor thermal comfort. *Int. J. Environ. Sci. Technol.* **2025**, *22*, 14975–14992. [CrossRef]
114. Pritipadmaja; Garg, R.D.; Sharma, A.K. Assessing the cooling effect of blue-green spaces: Implications for urban heat island mitigation. *Water* **2023**, *15*, 2983. [CrossRef]
115. Feng, H.; Feng, L.; Huang, F.; Sun, J.; Chen, J. Synergistic cooling effects of urban blue-green spaces at microscale: Using the synergistic cooling composite index. *Sustain. Cities Soc.* **2025**, *131*, 106768. [CrossRef]
116. Chen, L.; Zhang, Z.; Ewers, B.E. Urban tree species show the same hydraulic response to vapor pressure deficit across varying tree size and environmental conditions. *PLoS ONE* **2012**, *7*, e47882. [CrossRef] [PubMed]
117. Zou, Z.; Yan, C.; Yu, L.; Jiang, X.; Ding, J.; Ding, J.; Qiu, G. Different responses of evapotranspiration rates of urban lawn and tree to meteorological factors and soil water in hot summer in a subtropical megacity. *Forests* **2021**, *12*, 1463. [CrossRef]
118. Takebayashi, H. Influence of urban green area on air temperature of surrounding built-up area. *Climate* **2017**, *5*, 60. [CrossRef]
119. Yahia, M.W.; Johansson, E.; Thorsson, S.; Lindberg, F.; Rasmussen, M.I. Effect of urban design on microclimate and thermal comfort outdoors in warm-humid Dar es Salaam, Tanzania. *Int. J. Biometeorol.* **2018**, *62*, 373–385. [CrossRef] [PubMed]
120. Li, H.; Zhao, Y.; Wang, C.; Ürge-Vorsatz, D.; Carmeliet, J.; Bardhan, R. Cooling efficacy of trees across cities is determined by background climate, urban morphology, and tree trait. *Commun. Earth Environ.* **2024**, *5*, 754. [CrossRef]
121. Liu, Z.; Brown, R.D.; Zheng, S.; Jiang, Y.; Zhao, L. An in-depth analysis of the effect of trees on human energy fluxes. *Urban For. Urban Green.* **2020**, *50*, 126646. [CrossRef]
122. Rahman, M.A.; Stratopoulos, L.M.; Moser-Reischl, A.; Zölch, T.; Häberle, K.-H.; Rötzer, T.; Pretzsch, H.; Pauleit, S. Traits of trees for cooling urban heat islands: A meta-analysis. *Build. Environ.* **2020**, *170*, 106606. [CrossRef]
123. Yin, Y.; Li, S.; Xing, X.; Zhou, X.; Kang, Y.; Hu, Q.; Li, Y. Cooling benefits of urban tree canopy: A systematic review. *Sustainability* **2024**, *16*, 4955. [CrossRef]
124. Canal & River Trust. 5 Trees to Find on Your Canal Walk. 2025. Available online: https://canalrivertrust.org.uk/things-to-do/canal-and-river-wildlife/a-spotters-guide-to-waterway-wildlife/identifying-wildlife/5-trees-to-find-on-your-canal-walk (accessed on 12 July 2026).
125. White, M.P.; Elliott, L.R.; Gascon, M.; Roberts, B.; Fleming, L.E. Blue space, health and well-being: A narrative overview and synthesis of potential benefits. *Environ. Res.* **2020**, *191*, 110169. [CrossRef] [PubMed]
126. Canal & River Trust. Government Funding Cuts Put Future of Nation's Historic Canals at Risk. 10 July 2023. Available online: https://canalrivertrust.org.uk/news-and-views/news/government-funding-cuts-put-future-of-nations-historic-canals-at-risk (accessed on 31 July 2026).